Assessment of mathematical models for ultrafiltration of multi-solute continuous cross-flow process

by

Maysoon Ahmad

A thesis
presented to the University of Waterloo
in fulfillment of the
thesis requirement for the degree of
Master of Applied Science
in
Chemical Engineering

Waterloo, Ontario, Canada, 2012

AUTHOR'S DECLARATION

I hereby declare that I am the sole author of this thesis. This is a true copy of the thesis, including any required final revisions, as accepted by my examiners.

I understand that my thesis may be made electronically available to the public.

Maysoon Ahmad

Abstract

In recent years, ultrafiltration membrane-based technology has received increasing attention and great importance for water and waste water treatment. Different mathematical models are proposed to analyze and predict the permeate quality and flux during ultrafiltration of multi-solute solutions. These models are obtained from the literature and are classified into two broad categories: (i) simplified models developed from the assumption that the flux decline is controlled by a single mechanism only such as (a) osmotic pressure controlled, (b) gel layer controlled and (c) resistance in series models, (ii) advanced models that describe the flux decline and permeate quality during UF as a cumulative effect of several mechanisms. Therefore, the models range from simple analytical closed-form solutions (with the fewest parameters) to complex systems of ordinary equations (ODEs) that require the use of a numerical solver. The main purpose of this study is to conduct a thorough assessment of important flux decline models that can be found in literature. The ultimate goal of this analysis is to choose the model that is both easy and reliable. Such analysis is well supported by the experimental data of permeate quality and flux from literature where the separation of POME (carbohydrate constituents, crude protein and ammonia) in continuous cross-flow ultrafiltration process is used as an example for this study.

Preliminary results demonstrate that ultrafiltration models that don't explicitly account for multiple solutes system seem to give accurate prediction of flux decline during the early stages of ultrafiltration. However, the discrepancy between experimental data and the simulation becomes larger as flux approaches steady-state level.

Acknowledgments

Here I would like to express my genuine gratitude and appreciation to all persons who endlessly supported, assisted and helped me towards achieving my researches goals.

I would like to express my special appreciation to my mother for her trust and prayers. I would like to acknowledge the dedication and sacrifice of my husband and my kids. The thesis would have never been completed without my husband presence beside me.

I would like to express my genuine appreciation to my most respectful main supervisor Prof. Ali Elkamel for his inspiration and enthusiasm throughout this research work. It was a great pleasure to me to conduct this research under his constructive comments. My thanks go to my co-supervisor Dr. Rand Elshereef. I also would like to thank Professor Luis Ricardez and Professor Aiping for their helpful comments and suggestions. The greatest appreciation goes to all the staff of the School of Chemical Engineering for their full cooperation.

Table of Contents

List of Figures

List of Tables

List of Symbols

		Unit
D	Diffusivity	(cm^2/s)
C_g	Total concentrations of solutes in the gel layer	(kg/m^3)
C_b	Total concentrations of solute in the bulk	(kg/m^3)
C_p	Total concentrations of solute in the permeate	(kg/m^3)
A	Effective area for filtration	(m^2)
H	Effective filtration thickness	(m)
l_p	Specific permeability	
J_v	Volume flux of permeate	($m^3/m^2.s$)
$J_{v,ss}$	Volume flux of permeate at the steady-stat condition	($m^3/m^2.s$)
R_m	Resistance due to the membrane	(m^{-1})
R_g	Gel layer resistance	(m^{-1})
R_H	Hydraulic resistance	(m^{-1})
K_b	Total back transport coefficient	(m^2)
M_{bt}	Total back transport mass up to time t	(kg)
k	Mass transport coefficient	(m/s)
N	Number of parameters	

n	Total number of solutes	
P_m	Permeability coefficient	(m^2)
V_p	Total volume of permeate up to time t	(m^3)
V_g	Total volume of gel layer up to time t	(m^3)
V_p	Total volume of permeate up to time t	(m^3)
R	True rejection	
R o	Observed rejection	
t	Filtration time	(s)
v	Superficial velocity	(m/s)
z	Gel layer thickness	(m)

Greek letters

Δπ	Osmotic pressure difference across the membrane	(bar)
μ	Viscosity of the bulk	(Pa s)
Δp	Transmembrane pressure	(bar)

CHAPTER 1

Introduction

1.1. Membrane Technology

The last two decades have seen a significant development in membrane technology as a well-known separation process applied in different industries. The efficiency as well as the economics of the various industrial processes can be greatly improved if membrane processes are suitably integrated in the exiting process, particularly, where fractionation of a set of components is more desired than total conversion or separation (Chaturvedi et al, 2001). Membrane technology is playing an increasingly important role in the treatment of water and wastewater, since it uses least amount of energy and it works without the addition of any chemicals.

The last 30 years have seen the introduction of a range of membrane based separation units, in an attempt to supplement or replace techniques of distillation, adsorption, extraction and crystallization (Scott, 1996). There are different major types of Membrane technology included, microfiltration (MF), ultrafiltration (UF), nanofiltration (NF) and reverse osmosis (RO). They differ from each other mainly in pore size of the membrane used. Pore sizes in

membranes (or alternately described by molecular weight cut-offs, MWCO) can vary from 0.1 to 5000 nanometres (nm) depending on filter type. For Microfiltration membrane process which is used to separate suspended particles and colloidal particles the range of pore size is 0.1-10 microns.

For the Ultrafiltration membrane process, the pore size typically ranges from 0.1 to 0.001 micrometers. For Nanofiltration membranes which have the very smallest pore size, have a pore size in the order of nanometers. Membrane applications can be divided into: (i) concentration of species of interest (e.g. water removal from all other components); (ii) clarifications (i.e. separating suspended particles and colloidal from dissolved components) and (iii) component separations based on molecular size or any other physicochemical parameters. (Figure 1.1).

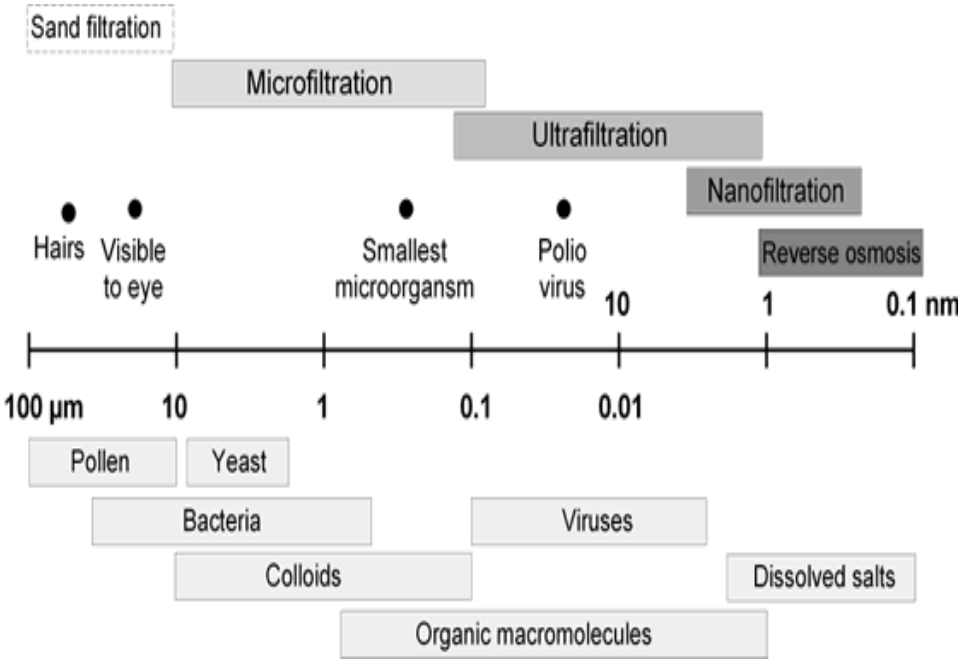

Figure (1.1): The different major types of Membrane technology; (http://www.memos-filtration.de/cms/en/membranfiltration.php).

1.2. Ultrafiltration Membrane:

Ultrafilltration is a membrane separation process using membranes with pore sizes between 0.1-0.001microns. It is used for the separation of suspended solids, colloidal materials, bacteria, virus and other pathogens which can impart color, tastes, and odors to the water and react with disinfectants to form disinfection byproducts (DBP) (Sadiq,2004). It is a pressure driven membrane process in which a membrane made of polymeric material fractionates components of a liquid as a function of their solvated size and structure which means that molecules larger than the membrane pore size rating will be retained

at the surface of the membrane so for all ultrafiltration applications the primary basis for separation is the molecular size (Catalina, Cot, Celma and Manich, 2009) as illustrated in Figure 1.2. The typical driving pressures to force the solvent to flow through the membrane are in the range of 10 to 100 psi (Joseph, Shen, Relond, and Probstein,(1977)).

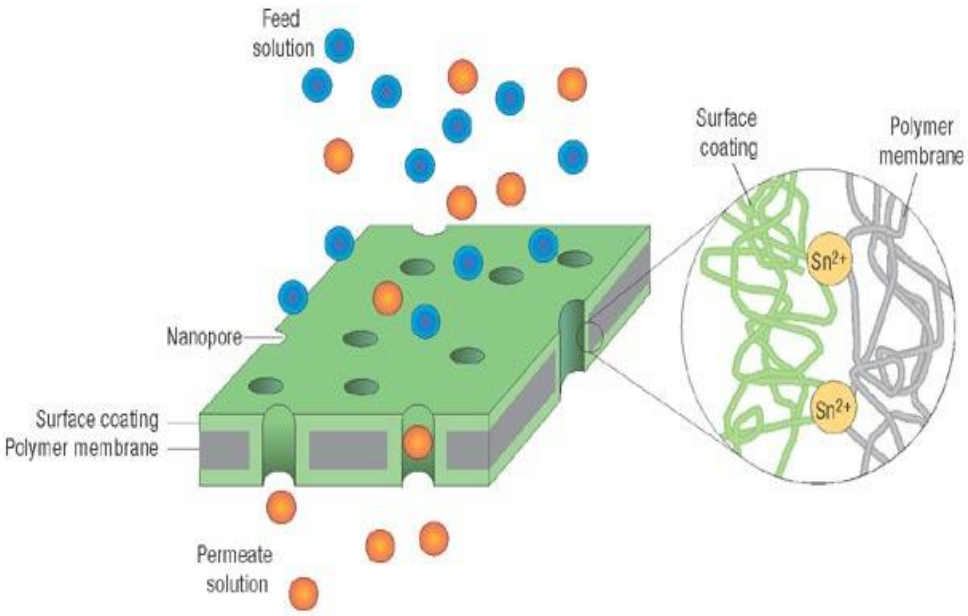

Figure (1.2): a membrane made of polymeric material that fractionates components of a liquid as a function of their solvated size and structure. (http://www.nature.com/nnano/journal/v3/n2/fig_tab/nnano.2008.13_F1.html).

1.3. Advantages of Ultrafiltration:

Membrane filtration has a number of benefits over the existing water purification techniques (www.lenntech.com/membrane-technology.htm):

1) The permeate is almost independent of feed water quality with high quality (clear without haze and germ).

2) Good removal efficiency towards bacteria and viruses.

3) There is no or less need of chemical agents.

4) It is simple and safe to operate and manage; also the process can be easily expanded.

5) It is considered to be a "Single step process", i.e. compact systems with well-arranged process conductions. In addition, it is easy to install and easily automated which allows low cost.

6) It produces highest quality water for least amount of energy. The energy that is used is minor compared to other techniques. Most of the energy that is required in ultrafiltration is used to pump liquids through the membrane.

7) For the Maintenance it is cheap and easy.

8) Excellent filtration performance with high flux.

9) In order to improve the ultrafiltration system performance, the fouling layer can be removed by using back washed and air scoured witch will extend the operating life for the system.

10) High chemical resistance and UF can be performed either at room temperature or in a cold room. This is mainly important because it enables

the treatment of heat- sensitive matter. That is why these applications are widely used for food production.

1.4 Applications of ultrafiltration membrane technology:

In recent years, ultrafiltration membrane technology has received increasing attention and great importance for water and waste water treatment for the removal of dissolved solids, color, and hardness in drinking water to produce water with very high purity and low silt density. Such application is becoming increasingly popular during the past decade and more cost effective.

Ultrafiltration is also used in a wide range of industrial applications including chemical food and beverage processing, pharmaceutical production, biotechnology, semiconductor manufacturing and dairy industries for process applications directly generating commercial products.

The common features of different ultrafiltration applications are summarized under the following applications:

Water treatment

- Treatment of groundwater and surface water to make drinking water and process water.
- Sterile filtration of drinking and beverage water.

- Producing pure water, ultrapure water and RO water for electronics industry.
- Producing pure water (bacteria free) for cosmetic and beverage use.

Waste water Treatment

- Removal of metal hydroxides from wastewater (Molinari el al.2004).
- Treatment of Oil emulsion wastewater.
- Treatment of wastewater containing sugar and oil/fat.
- Treatment and reclamation PVA in textile industry.
- Combination of separation processes and integrated process systems to treat all kinds of wastewater (reference?)..

Ultrafiltration also plays an important role in the following industries:

Machining industry

- Separation of highly stable oil / water emulsion's.

Pulp and Paper industry

- Treatment of bleach plant effluents.
- Reduce effluent load & reuse the water.

Fertilizer industry

- Recycling cooling tower blow down water.

Medical industry

- Remove the pyrogens from the water for the injections.
- Separation and harvesting of enzymes and pharmaceutical products.
- Purification of antibiotics and interferon.

Petroleum industry

- By removing the colloidal particles and the suspended solids from the refinery effluent.

Chlor alkali industry

- For the brine purification of the brine.

Textile industry

- Reduces sludge formation.
- Separate and recover the dye path and the associated rinses.
- Recovers salt for reduces salinity in the effluent.

Food industry

- Concentration of whey proteins and Gelatin.

- Recovery of sugar from sugary water.
- Heat sensitive proteins concentration for food additives.
- Whey treatment and concentration of skim milk in dairy industries.
- Potato protein recovery, egg and animal blood processing.
- Concentration and clarification of sugar juice.

1.6 Problem statement

One of the major problems confronting the use of ultrafiltration membrane in the industrial application is the multiple solutes system since the models proposed in the literature are only suitable to predict the performance of ultrafiltration with the single solute system and when we have multiple solutes system these models that can be found in the literature can only predict the total permeate concentration of the system and not for each individual solute.

However, for the multiple solutes system present the performance of ultrafiltration multiple solutes systems cannot be fully accessed in the literature since a small number of publications have been devoted.

Therefore, It is a problem to find and to choose the model that is suitable to analyze and predict the permeate quality and flux during ultrafiltration of multi-solute solutions.

1.6 Goals and Objectives of this Thesis:

The objectives of this thesis are stated as following:

1) Analysis and Comparisons of different mathematical models with the experimental data from the literature.
2) Analysis and comparisons between two advanced models from the literature. The first model was (Ahmad et al., 2006) model and the second model was a unified model (Bhattacharjee et al., 1996)
3) Investigate the effect of varying the key parameters of the process on the ultrafiltration dynamics and on the volume flux of permeate under different operating conditions

Such analysis is well supported by the experimental data of permeate quality and flux from literature where the separation of POME (carbohydrate constituents, crude protein and ammonia) in continuous cross-flow ultrafiltration process is used an example for this study.

1.7 Organization of the Thesis:

This thesis comprises of six chapters, including the introduction:

- **Chapter 2** presents a literature review on experimental and theoretical studies of ultrafiltration modeling of multiple solutes system for continuous cross-flow process.
- **Chapter 3** presents the experimental data obtained from the pilot plant scale membrane system with the pretreated palm oil mill effluent (POME) as the feed into the ultrafiltration model. A general overview of the experimental procedure, ultrafiltration data, observations and conclusions of these studies were introduced as well.
- **Chapter 4** deals with the modeling of ultrafiltration that contains a mathematical formulation of ultrafiltration and a detailed discussion of the similarities and differences between various ultrafiltration models. The validity of models has been tested by comparing the experimental data presented in Chapter 3 with theoretical predictions.
- **Chapter 5** investigate the effect of varying membrane parameters on the volume flux of permeate via numerical simulations.
- **Chapter 6** includes the final conclusions of the most important points and discussion for possible future development and studies that can be undertaken in the field of modeling ultrafiltration of multi-solute systems.

CHAPTER 2

Literature Review

2.1 Introduction

In this chapter, we present a theoretical review of the literature that is relevant to modelling ultrafiltration processes. We first examine the background to modelling membrane separation processes, and how they have devolved and how research has been conducted. We look in particular at various models used to describe the ultrafiltration process, comparing and contrasting these different methodological modelling approaches in terms of their assumptions and their respective range of validity. Various theoretical studies have been proposed to describe the dynamics of flux decline in ultrafiltration of a feed solution containing one-solute specie as a simple case scenario (i.e. single-solute aqueous feed solution). Such efforts are not only the most simple, but also the most representative of all the studies proposed in this area. Much of literature in this chapter will be critical for the development of the modelling framework described in Chapter 4, where we examine the approach of modelling flux decline in ultrafiltration by treating the feed solution as multiple-solute feed solution instead of a single-solute feed solution. The validity of models has been

tested by comparing the experimental data presented in Chapter 3 with theoretical predictions as will be illustrated in Chapter 4 of this thesis.

2.2. Theory of Ultrafiltration:

Ultrafiltration is a pressure-driven membrane process by which macromolecular solutes are separated from the solvent. For the filtration of a pure solvent following a laminar flow behavior, the permeate flux changes with the mean transmembrane pressure can be described by Carman-Konzeny equation (Carman (1938)) as:

$$J = L_p \Delta P = \frac{\Delta P}{\mu R_m} \qquad (2\text{-}1)$$

Where J is the flux (volumetric rate per unit area), ΔP is the transmembrane pressure, L_p is the permeability coefficient of the membrane, μ is the solvent viscosity, and R_m is the hydrodynamic resistance of the membrane.

To describe the ultrafiltration in the presence of a solute, the new form of eq (2-1) can be written as (Bowen and Jenner):

$$J = \frac{\Delta P - \Delta \pi}{\mu R_{total}} \qquad (2\text{-}2)$$

Where $\Delta\pi$ is the osmotic pressure difference between the bulk solution and the permeate and R_{total} is the total resistance and it is the sum of all sub-resistances towards mass transport as described in more detail in the following sections.

2.2.1 Concentration polarization

Concentration polarization is a very important phenomenon that describes how the accumulation of solutes retained by the membrane result in gradual build-up of fouling layer at the membrane surface with a relatively high concentration .This is because the retained solute cause the local concentration in the vicinity of the membrane to increase resulting in a concentration gradient as illustrated in Fig (2.1).

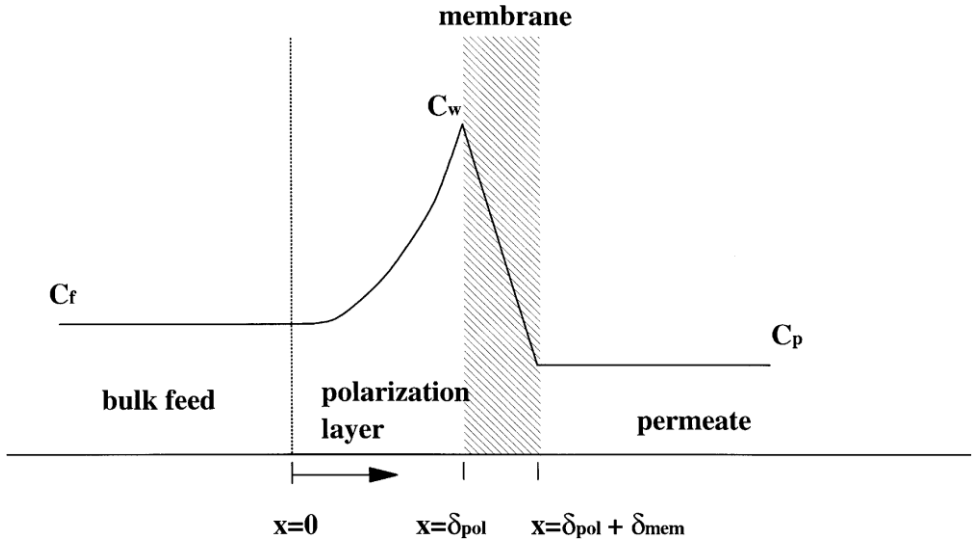

Fig(2.1): Schematic diagram of the concentration polarization boundary layer.

The accumulation of solute at the membrane surface will cause a diffusive back transport from the membrane toward the bulk of the feed, −D.dC/dy. The process reaches steady state when the convective transport of the solute towards the membrane surface is equal to the sum of the permeate flow plus the rate of the solute due to back-diffusion (Bowen and Jenner (1995))

$$Jc = D\frac{dc}{dy} + Jc_p \qquad (2\text{-}3)$$

c is the solute concentration in the boundary layer , c_p the solute concentration in the permeate and D is the diffusion coefficient.

The boundary conditions are

y=0→ c= c_m

y=δ → c = c_b

Integration of Eq. (2-3) results in the following equation

$$J = k_s \ln\left(\frac{c_m - c_p}{c_b - c_p}\right) \qquad (2\text{-}4)$$

This is the basic equation for concentration polarization (film model) where $k_s = D/\delta$, the overall mass transfer coefficient of the solute in the boundary

layer, and C_m is the concentration at the membrane surface and δ is the boundary layer thickness.

Several models have been developed to describe the polarization phenomena; in general they can be divided into three categories: gel-polarization model, osmotic pressure model and resistance in-series model as explained in the following sections:

2.3. Gel-polarization model:

Many investigators (Blatt el al.(1970), Porter (1972a,b), Henry (1972), Kozinski and Lightfoot (1972) and Fane et al. (1981) found that as the applied ultrafiltration pressure is increased, permeate flux first increases and then remains more or less pressure independent. At the end, a limiting flux is reached where further increase in applied pressure will result in slight increase in permeate flux. Such flux action was not explained well by the film model of concentration polarization (Jonsson1986).

This phenomenon was first explained by Michales (1968) and Blatt et al.(1970) who have been commented upon the gel polarization model. They found that as the solute concentration at the membrane surface increases to a very high value which will result in reaching its solubility limit, precipitation occurs on the membrane surface to form solid gels. Moreover, they concluded

that once the pressure increases to reach a value above a certain limit, this temporary increase in flux will lead to form a gel layer at the membrane surface. Steady state is attained when the hydraulic resistance of the gel layer causes a decrease in the permeate flux to the limiting value.

The gel concentration depends on the shape, size and chemical structure of solvation .On the other hand, it is independent of the applied pressure, bulk solution concentration and membrane characteristics (Marce (1996)).Michales's hypothesis assumes that as the applied pressure is increased further, the flux will increase temporarily, which in turn, will lead to bring more solute to the gel layer and increases its thickness, thereby the flux begins to drop below its original level due to the formation of gel layer of rejected particles on the membrane surface (Marcel (1996)).

Due to concentration polarization, the concentration of the solute at the membrane surface, (C_m), is much higher than that in the bulk solution and when (C_m) reaches a certain level, a gel layer will be formed with a gel layer concentration C_g . By assuming a complete solute rejection of 100% and neglecting the influence of concentration profile and permeate flux on the mass transfer coefficient, k_s, (2-4) can be simplified to the gel layer model equation:

$$J_{\lim} = k_s \ln\left(\frac{c_g}{c_b}\right) \qquad (2\text{-}5)$$

The gel-layer model equation (2-5) can be used to calculate the limiting flux ($J_{\lim}$) when the gel layer is formed.

Where $J_{\lim}$ the limiting is flux and C_g is the gel layer concentration.

Later, many investigators Porter (1972a, Henry (1972) and Madsen (1977) and others have supported the gel–polarization model by conducting ultrafiltration experiments to measure the limiting flux at different conditions.

From Equation (2-5), the following findings about the limiting flux can be directly deduced:

$J_{\lim}$ is independent of applied pressure

$J_{\lim}$ is semi-logarithmically related to C_b

$J_{\lim}$ approaches zero at a limiting bulk concentration $c_{b.\lim}$ which is equal the gel concentration c_g (or the cake-concentration in the case of colloidal dispersions)

$J_{\lim}$ may be modified by factors which alter the overall mass transfer coefficient.

2.4. Osmotic pressure model

As mentioned previously, the rejected solutes by the membrane accumulate near the membrane surface and this is known as the concentration polarization. The effect of this phenomenon will lead to extra hydraulic resistance to the solvent flow. Meanwhile, the osmotic pressure develops and acts against the applied transmembrane pressure.

Kedem and Katchalsky (1958) derived the osmotic pressure model by taking into account the osmotic pressure at the membrane surface as described in the following flux equation:

$$J = \frac{|\Delta p| - |\Delta \mu|}{\mu R_m} \qquad (2\text{-}6)$$

Where R_m is the membrane resistance and $\Delta\pi$ is the difference in osmotic pressure across the membrane (i.e. $\Delta\pi = \pi(c_m) - \pi(c_p)$) .From eq. (2-6), we notice that the osmotic pressure model assumes that the flux decline is a function of all operating variables including the transmembrane pressure P. This is different from the gel polarization model which describes the flux decline as a function of mass transport coefficient across the membrane as well as concentration solute at the membrane while ignoring the influence of pressure drop across the membrane.

Generally the osmotic pressure represented in terms of a polynomial rather than linear and can be described by the following equation:

$$\pi = a.n^{c} \qquad (2\text{-}7)$$

Where a is a constant and n is an exponential factor with a value greater than 1.

An interesting analysis of the osmotic pressure model was provided by Wijmans et al.(1984).

Assuming complete rejection ($c_p = 0$), the osmotic pressure π can be expressed as

$$\Delta\pi = \pi(c_m) = ac_m^n \qquad (2\text{-}8)$$

With n>1. C_m is dependent on permeate flux according to Eq.(2-4), which gives

$$J = \frac{|\Delta p| - ac_b^n \exp(nJlk_s)}{\mu R_m} \qquad (2\text{-}9)$$

Wijmans et al.(1984) clearly showed how the derivatives of Eq.(2-9) provides insight into the ultrafiltration process. So the flux-pressure derivative becomes

$$\frac{\partial J}{\partial|\Delta p|} = \left[\mu R_m + \frac{n}{k_s}(|\Delta p| - J\mu R_m)\right]^{-1} = \left[\mu R_m + \frac{n}{k_s}|\Delta\pi|\right]^{-1} \qquad (2\text{-}10)$$

Given the asymptotes

$$\frac{\partial J}{\partial |\Delta p|} \to (\mu R_m)^{-1} \qquad \text{for } |\Delta p| \to 0 \text{ , or } |\Delta \pi| \to 0$$

and

$$\frac{\partial J}{\partial |\Delta p|} \to 0 \qquad \text{for } |\Delta p| \to \infty \text{ , or } |\Delta \pi| \to >> J\mu Rm$$

Similar to the gel- polarization model, the flux- pressure profile start at low Δp with the same slope as pure solvent flow and when Δp increases the slope will decline and approaches zero at high pressure .

Rearranging Eq.(2-9), taking the logarithm and differentiating to give the following Eq.

$$\frac{\partial J}{\partial \ln c_b} = -\left[\frac{1}{k_s} + \frac{1}{n\left(\frac{|\Delta p|}{\mu R_m} - J\right)}\right]^{-1} = -k_s\left[1 + \frac{\mu R_m k_s}{n|\Delta \pi|}\right]^{-1} \qquad (2\text{-}11)$$

Which shows that when polarization is significant, that is,

$|\Delta p| >> J\mu\ Rm$ or

$$\frac{n|\Delta \mu|}{\mu R_m k_s} >> 1,$$

Then

$$\frac{\partial J}{\partial \ln c_b} \to -k_s$$

The limiting concentration $C_{b,\lim}$ for J→0 is obtained from equation (2-9) when

$$\Delta p = a c_{b,\lim}^{n} = \pi(c_{b,\lim}) \qquad (2\text{-}12)$$

Which gives an osmotic pressure equal to the applied pressure.

The conclusion from the Wijmans et al. (1984) theoretical analysis is that,

1. As the membrane resistance Rm decrease this will cause a more pronounced osmotic pressure effect, that is flux limitation at lower applied pressures.
2. As the osmotic pressure increases , the bulk concentration will increase too ,hence the osmotic pressure limitation will be expected in ultrafiltration of medium macrosolutes (10^4-10^5 Mwt).

2.5 Resistance models

To obtain the resistance –in-series relationship, neglect the osmotic pressure term in equation (2.2).

$$J = \frac{|\Delta p|}{\mu R_{total}} \qquad (2\text{-}13)$$

Where R_{total} is equal to the summation of R_m (the membrane resistance) and R_s (the solute resistance). Using the filtration theory, the polarized solids resistance equation is

$$R_s = \alpha \frac{m_p}{A_m} \qquad (2\text{-}14)$$

Where m_p is the mass of the deposited particles, A_m is the membrane area and finally α is the specific resistance of the deposit particles and it is related to the spherical particles properties by using Carman – Konzeny relationship (Carman (1938))

$$\alpha = \frac{1800(1-\varepsilon)}{\rho_p d_p^2 \varepsilon^3} \qquad (2\text{-}15)$$

Where ρ_p and d_p is the density and the mean diameter of the particles respectively and ε is the void volume of the cake.Equations (2-12),(2-13) and (2-14) apply very well for colloidal ultrafiltration (Faane (1984)).

A general observation would be that in case of unstirred dead-end ultrafiltration for constant pressure conditions and with no particle pack transport, R_s will increase with time since

$$m_p \equiv Vc_b \qquad (2\text{-}16)$$

Where V is the total volume filtered.

By integrating the following Equation

$$J = \frac{dV}{A_m dt} \qquad (2\text{-}17)$$

And a combination of Equations (2-13),(2-14) and (2-16) this will lead to the well –known constant pressure filtration equation and it was first suggested by Underwood (1926)

$$\frac{t}{V} = \frac{\mu R_m}{A_m |\Delta p|} + \frac{\mu \alpha c_b}{2 A_m^2 |\Delta p|} V \qquad (2\text{-}18)$$

The result of plotting the above equation (experimental data of t/v versus V) yields a straight line which will help in determine both α and R_m

The resistances which can occur during the ultrafiltration are:

1. R_m, is the resistance of the membrane.

2. R_p, is a resistance due to pores blocked by the solute .

3. R_a , adsorption of the solute on to the membrane surface .

4. R_{cp}, an additional resistance occur because of the concentration polarization

R_g, is the gel resistance. The gel layer formation occurs as mentioned before, when the concentration at the membrane surface reach high values that the concentrated solution will change into a gel with a resistance Rg.

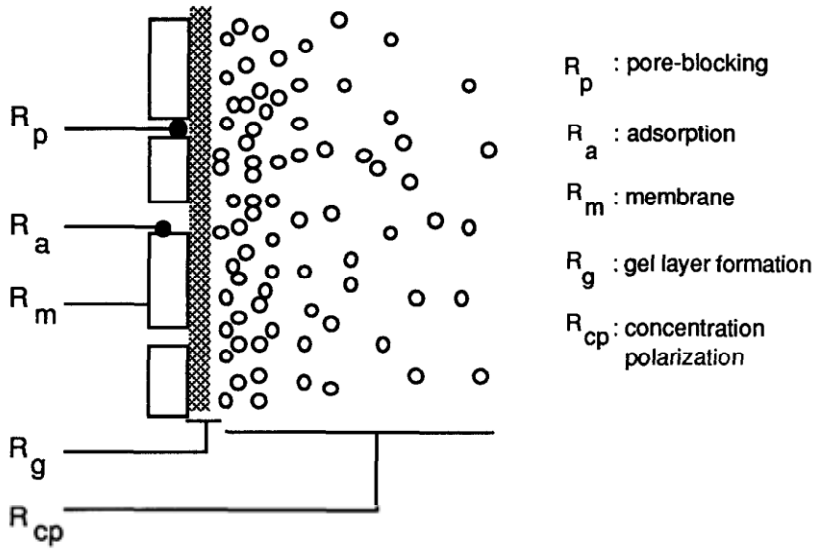

Fig(2.2) : Possible resistance against solvent transport.

2.5.1 Gel-Polarization Resistance Model

In terms of resistances, Fan(1956) expressed the gel-polarization model on the following equation

$$J = \frac{|\Delta P|}{\mu(R_m + R_{bl} + R_g)} \qquad (2\text{-}19)$$

Where R_g is the gel layer resistance at limiting concentration (c_g). R_{bl} is the resistance of the boundary layer. Now, when the pressure increases, the concentration polarization increases from zero to the gel concentration (c_g) and this will lead to $(R_g = 0)$ as a result the flux is depend on the pressure. After the

formation of the gel layer, R_g is established and the thickness of the gel layer will increase with increasing the transmembrane pressure as a result the flux will be independent of the pressure.

To describe the dynamics of polarization in stirred or cross- flow ultrafiltration Chudacek and Fane (1984) used the filtration model .The new form of the resistance model (Eq.(2-11))

$$J = \frac{\Delta P}{\mu(R_m + R_s + R_{sr})} \qquad (2\text{-}20)$$

Where R_s is the resistance which produced by deposition of all convectively transported solute, and R_{sr} is the resistance removed by stirring or cross – flow.

Chudacek and Fane assumed the following assumption regarding the back transport:

1. The back transport is constant.
2. The back transport is equal to the convective solute transport at steady state (J_{ss} C_b)

   Under the previous assumptions Eq.(2.16) is not any more valid and the new form of Eq.(2.20) will be

$$J = \frac{\left| \Delta P \right|}{\mu\left[R_m + (V / A_m - J_{ss} t)\alpha c_b \right]} \qquad (2\text{-}21)$$

In order to find *Jss* value , there are two methods either by using Eq.(4) (the model relationship) or experimentally determined α values and measured *Jss* quantity.

2.5.2 Boundary layer resistance model

The boundary layer resistance model for cross- flow ultrafiltration of dextran solutions was first proposed by Wijmans et al. (1985) where there are no gel-formation .The principle of boundary layer resistance model is the same as the sedimentation experiment where there is a correspondence of the permeability of a concentrated solute layer for solvent flow and the permeability of a solute in stagnant solution .Mijnlieff and Jaspers (1971) gave the following expression foe this relationship

$$P = \frac{\mu s}{c(1 - \frac{v_1}{v_o})} \qquad (2\text{-}22)$$

Where P is the permeability of a concentrated solute layer of concentration c, v_0 and v_1 are the partial specific volumes of both the solvent and the solute respectively .s is the sedimentation coefficient at concentration c and it can be described by the following expression

$$\frac{1}{s} = \frac{1}{s_0}(1 + K_1 c + K_2 c^2 + K_3 c^3) \qquad (2\text{-}23)$$

Where K_1, K_2 and K_3 are constants.

The hydrodynamic resistance of the boundary layer R_{bl} is described by

$$R_{bl} = \int_0^{\delta} r_{bl}\, dy \qquad (2\text{-}24)$$

Where r_{bl} is the specific resistance of the boundary layer.

The permeability is a function of the coordinate y perpendicular to the membrane since it depends on the concentration and there is a concentration profile in the boundary layer.

Thus , the boundary layer resistance is

$$R_{bl} = \int_{o}^{\delta} \frac{1}{p(y)} dy \qquad (2\text{-}25)$$

Substituting Eq.(2.22),(2.23) with $c(y) = c_b \exp(J_y / D)$ into Eq.(2.24)and integrating over the boundary layer thickness δ the new form of Eq.(2.25) will be

$$R_{bl} = \frac{D}{\mu s_o J}\left(1 - \frac{v_1}{v0}\right)\left[c_m - c_b + \frac{K_1}{2}(C_m^2 - c_b^2) + \frac{K_2}{3}(c_m^3 - c_b^3) + \frac{K_3}{4}(c_m^4 - c_b^4)\right]$$

(2-26)

Where c_m is the solute concentration at the membrane surface, which can be known in case if k_s is known by using the film model relationship (Eq.(2-4)).

Combining Eq. (2-13) with $R_s = R_{bl}$,(2-26) and Eq.(2-4) for $c_p = 0$ to obtain the boundary layer resistance model where the parameter flux is the single unknown parameter.

$$J = \frac{|\Delta P|}{\mu\left(R_m + \frac{D}{\mu s_o J}(1-\frac{v_1}{v_0})\left[c_m - c_b + \frac{K_1}{2}(c_m^2 - c_b^3) + \frac{K_2}{3}(c_m^3 - c_b^3) + \frac{K_3}{4}(c_m^4 - c_b^4)\right]\right)}$$

(2-27)

With

$$c_m = c_b \exp(J / k_s)$$

So in order to calculate the flux, the process conditions ($\Delta p, R_m, c_b, k_{s)}$ and the physical properties of the solute – solvent system (s,D) should be known .

Wijmans et al.(1985) ,calculated the mass transfer coefficient by applying the osmotic pressure model and after they proved that the osmotic pressure model and the resistance model are equivalent , they obtained an excellent agreement between their calculated and experimental flux values.

Nakao et al.(1986) examined the concentration polarization effect in unstirred ultrafiltration using the boundary layer resistance model adapted to the cake filtration theory to analyses the experimental flux behavior of dextran and polyethylene glycol solutions .Therefore a step concentration profile and a time –independent concentration in the boundary layer without any solute back – transport were assumed. It observed that the model worked well in predicting

the experimental flux behavior but it need several other experiments in order to obtain the necessary parameters.

Much of the literature in this chapter will be critical for the development of the modelling framework described in Chapter4, where we examine the approach of modelling flux decline in ultrafiltration by treating the feed solution as multiple-solute feed solution instead of a single-solute feed solution. The validity of models has been tested by comparing the experimental data presented in Chapter 3 with theoretical predictions as will be illustrated in Chapter 4 of this thesis.

CHAPTER 3

Ultrafiltration Experimental Data

Chapter 3 presents experimental data obtained from the literature. These experimental data will be used to test the validity of different models described in Chapter 4. The most important models that will be validated are the preliminary ultrafiltration models (gel-boundary layer controlled model, osmotic pressure controlled model as well as resistance model) and two advanced models represented by (i) ultrafiltration of multi-solute species and (ii) ultrafiltration of single solute specie. The discussion in Chapter 4 will be related to which model describes the experimental data better and what limitation each model has in general. The purpose of Chapter 3 is to present the reader to the type of experimental data that was obtained from literature and the conditions at which the experimental data was obtained. The experimental data presented in Chapter 3 are from a pilot plant scale membrane system with the pretreated palm oil mill effluent (POME) as the feed into the ultrafiltration module in order to separate the organic matters from the pretreated palm oil mill effluent. The POME was composed of ternary solutes system (carbohydrate constituents, crude protein and ammonical nitrogen). A general overview of experimental procedures, ultrafiltration data, observations and conclusions of these studies are briefly introduced as well.

3.1. Experimental Study:

Ahmad et al., (2006) carried out an experimental and theoretical study to develop a mathematical model to predict the performance of an ultrafiltration process in the separation of POME (multiple solute systems) in continuous cross-flow ultrafiltration. They developed model for both the prediction of the concentrations of each solute in the permeate and for prediction of the volume flux of permeate and gel layer resistance.

With the rapid expansion of the palm oil industry combined with increased environmental awareness and required, the final industry discharge should meet the standard discharge limit by treat its effluent to an acceptable level before discharge.

Palm oil mill effluent (POME) is wastewater generated from the palm oil milling process, is considered the most harmful waste for the environment if discharged untreated pretreatment due to its high chemical oxygen demand (COD).

POME is a ternary solutes system mixture of organic matters. The carbohydrate constituents comprise of low molecular weight monosaccharide (180 kg/kmol) to high molecular weight polysaccharide (400,000 kg/kmol) .The crude protein comprises from the simplest compounds of amino acids (75 kg/kmol) to the most complex compounds of proteins (450,000 kg/kmol).

Nitrogen in POME is originally present in the form of organic (protein) nitrogen, and as time progresses, the organic nitrogen is gradually converted to ammoniacal nitrogen which has the molecular weight of 17–35 kg/kmol. The transport of the organic matters (mainly carbohydrate constituents, crude protein andammoniacal nitrogen) through the ultrafiltration is very important. The transport of these organic matters will finally determine the COD and ammoniacal nitrogen concentration in the permeate (Ahmad et al., (2006)).

In Malaysia, palm oil is very productive where palm oil mills are operated at least 300 days per year(R. M. Kutty) .Under the Environmental Quality Act of Malaysia 1976 , The COD and ammoniacal nitrogen concentration of the final discharge should meet the standard discharge limit. Here is a description of their experimental study as given in their paper.

3.2. Sample preparation

Ahmad et al., (2006) obtained the POME from the United Palm Oil Mill, Penang, Malaysia. Since their purpose of pretreatment of POME is to remove the oil and grease and the solids before the POME is fed into the ultrafiltration system (Ahmad et al., 2003, 2005b) they first started with the coagulation and flocculation process. In contrast, hundreds of liters of POME was transferred to a chemical treatment tank and they purchased three liters of coagulant, modified industrial grade alum from Envilab Sdn. Bhd in order to added into the POME

at the stirring speed of 50 rpm. To adjust the pH value to the pH 6 they used industrial grade sodium hydroxide 65% (NaOH). They also added three liters of flocculant (0.1%), cationic polymer (FO 4190) the POME at the stirring speed of 10 rpm for 15 min. After that, they allowed the mixture allowed to settle and they removed the result sludge by using a filter press. The supernatant is the pretreated POME for ultrafiltration. Table 1 presents the characteristic of raw and pretreated POME. The details of the pretreatment of POME are presented elsewhere (Ahmad et al., 2003). Table(3.1) shows clearly that the oil and grease as well as the suspended solids were removed (with 70% removal of COD) by the coagulation and flocculation process. For the remaining COD (30%) it was removed by the ultrafiltration and reverse osmosis processes.

Table 3.1: Characteristic raw POME and the treated POME (Ahmad et al., 2006).

Parameter	Raw POME	Pretreated POME
PH	4.7	6.0
Oil and grease, mg/L	4000	Not detectable
Chemical oxygen demand (COD),mg/L	50,000	15,000
Suspended soilds, mg/L	40,500	Not detectable
Ammoniacal nitrogen, mg/L	35	34

The ultrafiltration in this case serves as the pretreatment for reverse osmosis. From the chemical composition analysis of the pretreated POME, the major components (solutes) contribute to the COD are carbohydrate constituents, crude protein and ammoniacal nitrogen (Hwang et al., 1978; Ho et al., 1984). Therefore, the pretreated POME forms a ternary solutes system for ultrafiltration. The pretreated POME samples at various concentrations were prepared by diluting the sample with distilled water. The details of the experimental run are listed in Table (3.2).

Table 3.2: Details of the experimental data (Ahmad et al., 2006).

Run	ΔP (bar)	Q_F (m3/h)	C_{total} (mg/L)	$C_{carbohydrate}$ (mg/L)	$C_{protien}$ (mg/L)	$C_{ammonia}$ (mg/L)	COD (mg/L)	Ro
1	1	4	5720	3015	2675	34	15,000	0.17
2	2	4	5720	3015	2675	34	15,000	0.21
3	3	4	5720	3015	2675	34	15,000	0.25
4	4	4	5720	3015	2675	34	15,000	0.26
5	4	3	5720	3015	2675	34	15,000	0.11
6	4	5	5720	3015	2675	34	15,000	0.41
7	4	7	5720	3015	2675	34	15,000	0.56
8	4	4	1431	754	669	8	3750	0.08
9	4	4	2862	1508	1337	17	7500	0.13
10	4	4	7155	3770	3344	42	18,750	0.33

ΔP = transmembrane pressure; Q_F =feed flowrae; C_{total} = total bulk concentration; $C_{carbohydrate}$ = bulk concentration for carbohydrate constituents ; $C_{protien}$ = bulk concentration for crude protein; $C_{ammonia}$ = bulk concentration for ammonical nitrogen ;COD =COD in the feed streame ; R_o = overall observed rejection.

3.3. Membrane system:

Fig. (3.1) shows a schematic diagram of their pilot plant scale equipment setup used in the present study. The ultrafiltration membrane was the ceramic membrane module P16-60 (PCI-Memtech) with housing constructed from stainless. The membrane module had a nominal molecular weight cut-off (MWCO) of 2500–10,000 g/mol with 19 flow channels. For each tube, the inner diameter and its length was 6.0mm and 1020 mm respectively. The filtration effective area was 0.36m2 and could be operated up to maximum pressure of 6 bar.

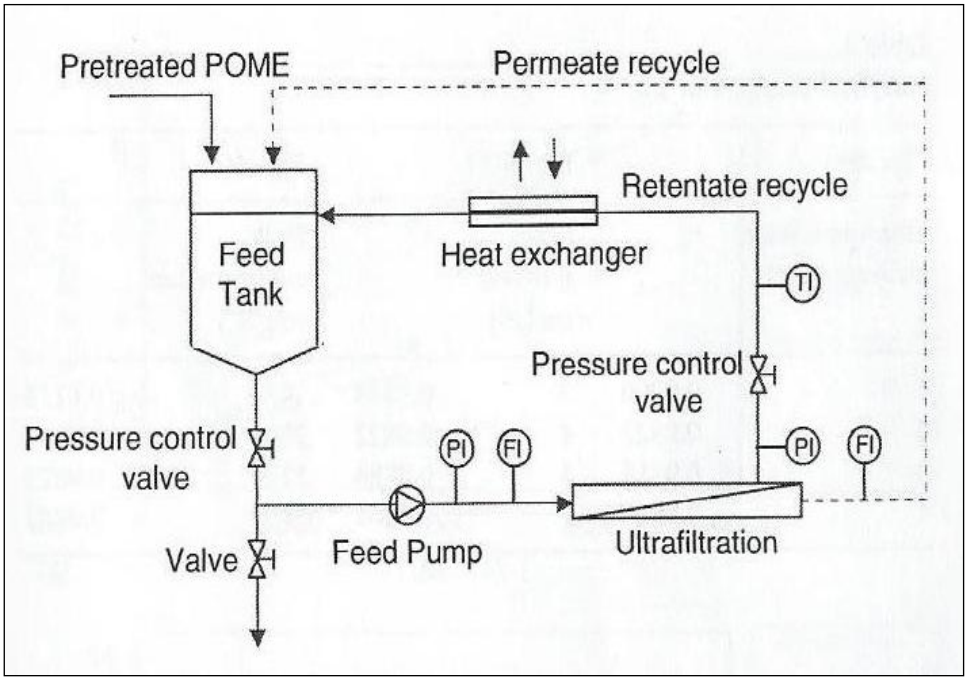

Figure (3.1): Schematic diagram of the pilot plant scale equipment set up for ultrafiltrationstudies. The symbol Pl is the pressure indicator,Fl is the flowmeter and Tl is the temperature indicator (Ahmad et al., 2006).

The pretreated POME was placed in the feed tank of the membrane system and by using water cool heat exchanger the temperature was maintained at (25 ◦C). The centrifugal pump (Grundfos CRN-8-50) was used to pump the feed through the membrane module. The required cross flowrate and transmembrane pressure were adjusted using pressure control valves (Gemu-diaphragm type) and the turbine function flowmeters (Burkert) were used to measure cross-flowrates of the feed and permeate. The pressure gauges were used to measure the inlet and outlet pressures of the module. In order to maintain a constant feed concentration the permeate and the retentate streams were recycled back to the feed tank (total recycle mode).

3.4. Analysis:

They used several methods and instrument in order to find the viscosity value and the concentration for each solute.

1. A Hoeppler falling ball viscometer was used to measure the viscosity.
2. The carbohydrate constituents were measured by using the colorimetric method with the phenol–sulfuric acid 98% reaction (Dubois et al., 1956).

3. For the crude protein it was determined by using the colorimetric method with a detergent-compatible formulation based on bicinchoninic acid (BCA Protein Assay, Pierce).
4. The ammoniacal nitrogen was measured by using the preliminary distillation step coupled with titrimetric method with standard sulfuric acid titrant, 0.02 N.
5. The colorimetric method at wavelength 600 nm with spectrophotometer CECIL 1000 series, Cambridge, UK (APHA, 1999) was used to measure COD.

3.4.1. Estimation of system Parameters:

Ahmad et al.(2006) estimated the parameters of μ, R_m , P_m , K_{bi} , K_i by using the experimental data in Figures (3.2),(3.3),(3.4),(3.5),(3.6) and (3.7).The method is mentioned in chapter(4) section (4.1.7) and (4.1.8) .The result are listed in (table 3.3) and it was in good correspondence with their typical value reported in the literature (Bhattacharjee and Datta, 2003; Karode, 2001; Mehta and Zydney, 2005).

1. Viscosity *(*μ*)* - Due to the presence of organic matter (carbohydrate constituents, crude protein and ammoniacal nitrogen) in the pretreated POME the viscosity *(*μ*)* of pretreated POME as 1.0240×10^{-3} Pa s was slightly higher than the viscosity of water *(*8.7790×10^{-4} Pa s*)*.

2. Membrane resistance *(Rm)* - The estimated value of membrane resistance *(Rm)* matched the typical value for ceramic membrane (Mehta and Zydney, 2005).

3. Permeability coefficient *(Pm)*-In this work the value of permeability coefficient *(Pm)* of the system depends on the both the type of solutes and the type of membrane used. However, the calculated value of magnitude value *(*10^{-16}) of *Pm* was in good agreement with the value reported in the literature (Bhattacharjee and Datta, 2003).

4. Back transport coefficient *(Kbi)*-For every each individual solutes the value *(Kbi)* estimated in this work was 10^{-8} m2 in contrast the typical value reported in the literature (Bhattacharjee and Datta, 2003) using continuous stirred ultrafiltration was 10^{-10} m2. The difference between the two values indicates that the turbulence created by continuous cross-flow ultrafiltration lead to higher back transport of the solutes compared to the turbulence created by stirred ultrafiltration. Since carbohydrate constituents had the largest molecular size compared to other solutes the estimated value for its back transport coefficient (*Kb*,carbohydrate) was higher than the other solutes.

5. Mass transfer coefficient (*ki)*- The calculated mass transfer coefficient value (*ki)* for every each individual solutes in the system was in good correspondence with the value reported in the literature (Bhattacharjee and Datta, 2003; Karode, 2001) and *ki* (2×10^{-6} -5×10^{-6} m/s), value matched with the volume flux of

permeate *(*5×10^{-6}–35×10^{-6} m/s*)* this will conclude that the gel polarization effect taken into consideration in the present work was valid.

Table 3.3: Estimated parameters obtained from experimental data (Ahmad et al., 2006).

Parameter		Value	
$\mu\ (10^{3}$ Pa.s)		1.0240	
$R_m\ (10^{-12}\ m^{-1}\ )$		2.1576	
$P_m\ (10^{16}\ m^{2})$		8.6464	
	Carbohydrate	Protien	Ammonical nitrogen
$K_{bi}\ (10^{8}\ m^{2})$	19.2414	4.3795	8.3812
$K_i\ (10^{6}$ m/s)	4.9940	2.9375	3.5777

The experimental data in Figures (3.2), (3.3), (3.4), (3.5), (3.6) and (3.7) will be used in Chapter 4 to test the validity of different mathematical models by comparing them to experimental data.

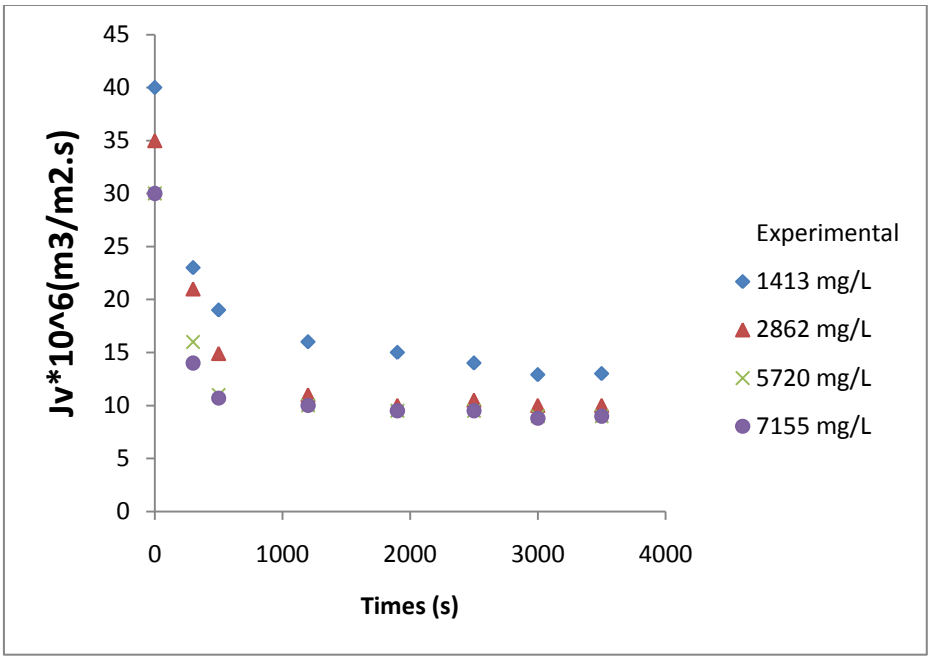

Figure (3.2): Experimental data for ultrafiltration experiments at four different concentrations. [Ahmad et al., (2006)].

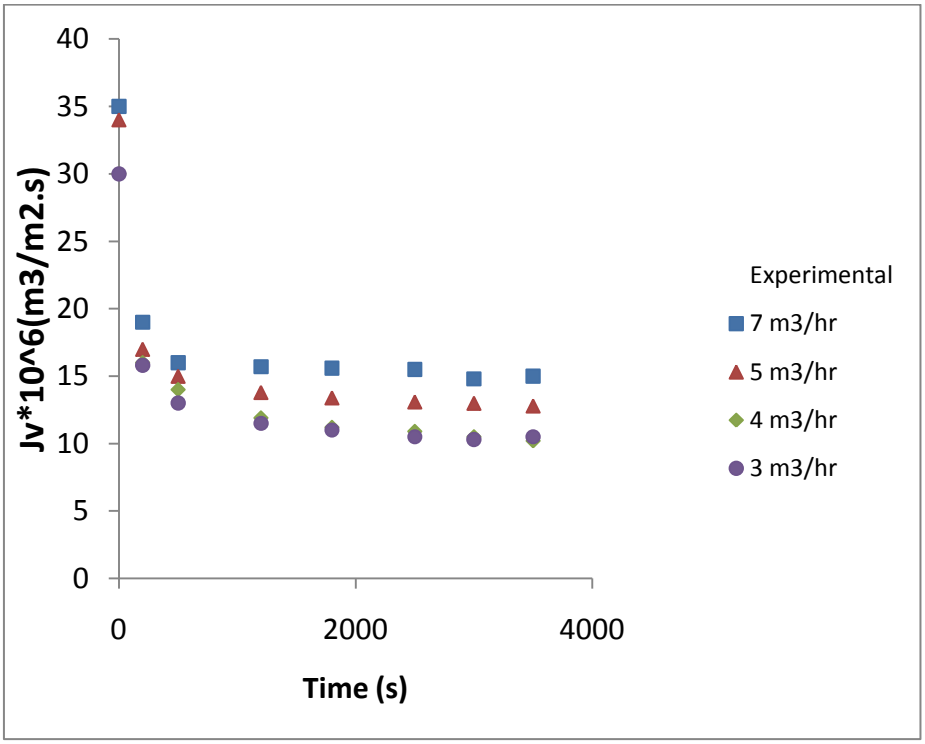

Figure (3.3): Experimental data for ultrafiltration experiments at four different flow-rates [Ahmad et al., (2006)].

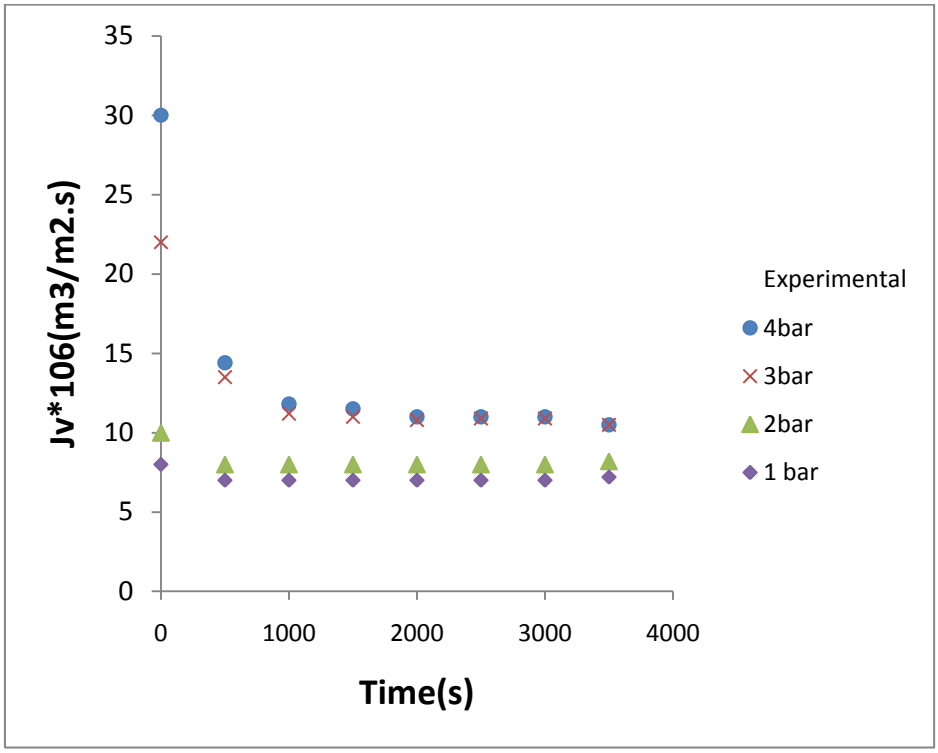

Figure (3.4): Experimental data for ultrafiltration experiments at four different transmembrane pressure [Ahmad et al., (2006)].

Figures (3.2), (3.3) and (3.4) indicates that the fouling of the membrane caused the volume flux of permeate to decrease until the system reached a steady-state value.

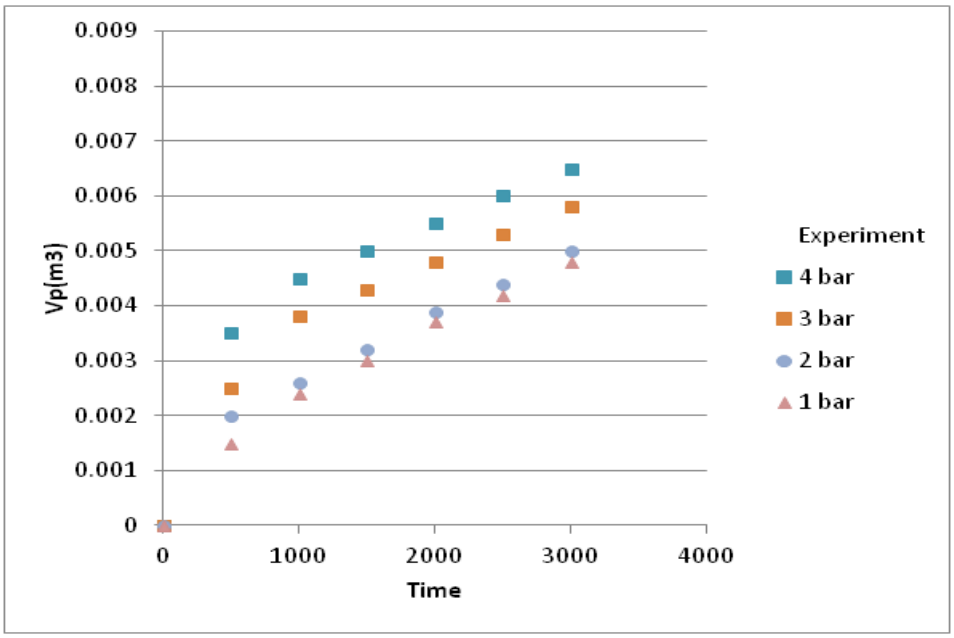

Figure (3.5): Total permeate volume against filtration time at different transmembrane pressure. [Ahmad et al., (2006)]**.**

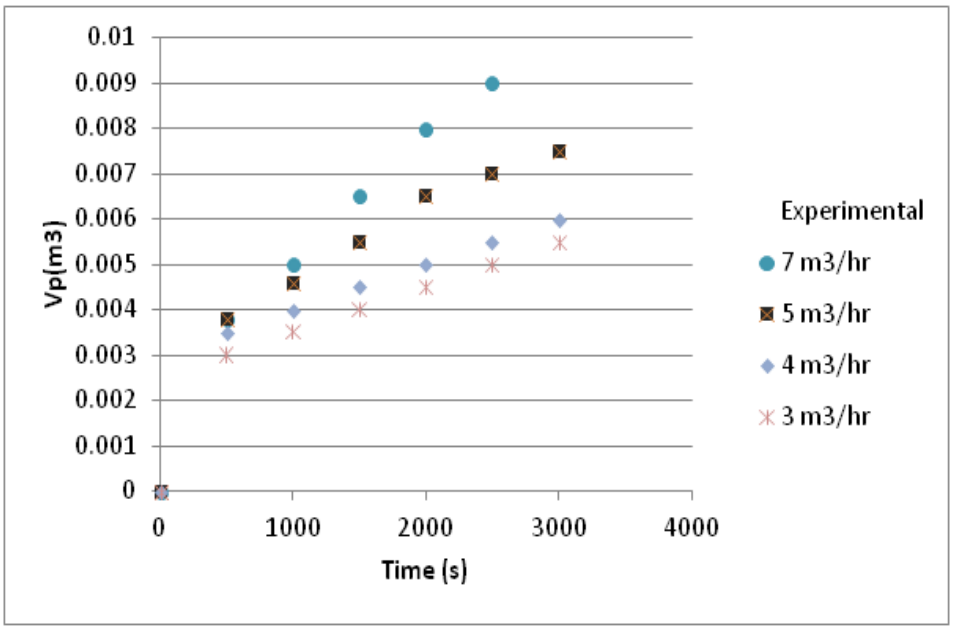

Figure (3.6): Total permeate volume against filtration time at different feed flowrate [Ahmad et al., (2006)]**.**

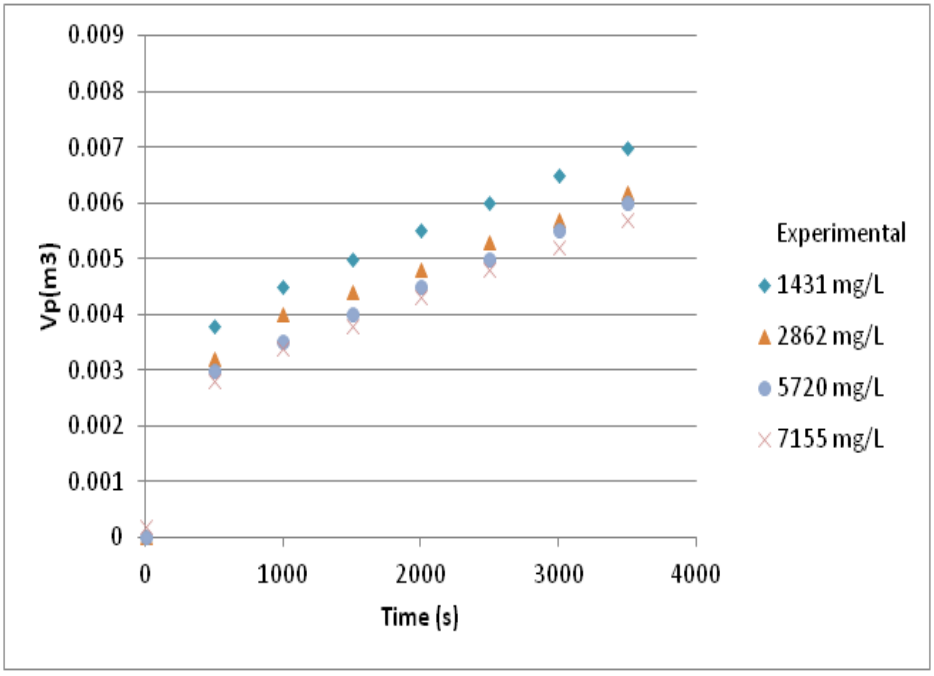

Figure (3.7): Total permeate volume against filtration time at different bulk concentration [Ahmad et al., (2006)]**.**

CHAPTER 4

Ultrafiltration Mathematical Models (Analysis and Comparisons)

The purpose of this chapter is to compare different mathematical models with the experimental data from the literature. This analysis is well supported by the experimental data from literature presented in Chapter 3. In this chapter, we present a theoretical review of literature that is relevant to modelling ultrafiltration processes. We have examined in Chapter 2, a general background to modelling membrane separation process, and how they have developed and how research has been conducted. We looked in particular at various preliminary models used to describe the ultrafiltration process, comparing and contrasting these different methodological modelling approaches in terms of their assumptions. Various theoretical studies have been proposed to describe the dynamics of flux decline in ultrafiltration of a feed solution containing one-solute specie as a simple case scenario (i.e. single-solute aqueous feed solution). Such efforts are not only the most simple, but also the most representative of all the studies proposed in this area. Much of literature in Chapter 2 was critical for the development of the modelling framework described in Chapter 4, where we examine the approach of advanced modelling of flux decline in ultrafiltration by treating the feed solution as multiple-solute feed solution (Ahmed et al,2006)

instead of a single-solute feed solution (Bhattacharjee and Datta,2003) as will be described in the following sections.

4.1. Development of the multi-solute filtration model (Ahmad et al., 2006):

An analysis of the flux decline encountered during ultrafiltration (UF) in a cross flow processes is presented by including the combined influence of the osmotic pressure resistance and the gel layer. A predictive model for prediction the volume flux of permeate in continuous cross-flow ultrafiltration processes is developed based on the mass balance analysis and by unifying the osmotic pressure, gel-layer resistance and gel polarization models. The present development model predictions match closely with the experimental flux behavior for all cases, while individual osmotic pressure, gel-layer resistance and gel polarization models are found to be inadequate. Let us start here with the overall mass balance over the multiple solutes system of continuous cross-flow ultrafiltration. The following simplifying assumptions have been made to the general problem formulation in Section 4.1.

In section 4.1.1, we begin by formulating, in rather general form the general mass balance equation over the multiple solutes system in the gel layer. Meanwhile the following sections (4.1.4.-4.1.7) present different mathematical models that provide a conceptual framework for understanding the phenomenon

responsible for flux decline for the multiple solutes system for continuous cross-flow system. Herein, the existing models have been arranged according to their complexity and the number of assumptions involved. Starting from section 4.2, which presents the simplest mathematical model of ultrafiltration (osmotic pressure model), the analysis has been extended by presenting more advanced models. The differences and similarities between models have been discussed in order to understand the connection and applicability between diverse treatments of the flux decline problem.

4.1.1. The mass balance in the gel layer:

The separation of solute and solvent takes place at the membrane surface where the solvent passes through the membrane and the rejected solutes deposited on the membrane surface .The deposited layer is termed as 'gel layer' and the concentration of each solute in the gel layer is termed as 'gel concentration'. With the higher concentration at the membrane surface and due to stirring action caused by the superficial velocity, there will be a tendency of some solutes to remove and diffuse back into the bulk (back transport effect) according to Fick's law of diffusion.

$$J = -DA\frac{dX}{dx} \qquad (4\text{-}1)$$

Ii is clear from the Ficks law that the flux (J) over a short distance dx is proportional to the driving force which is expressed as the gradient of X, over the distance (dx) perpendicular to the front area of the diffusion ,A. The proportionality constant is the diffusivity D (cm^2 / s). The sign convention means that the diffusion will be in the positive direction.

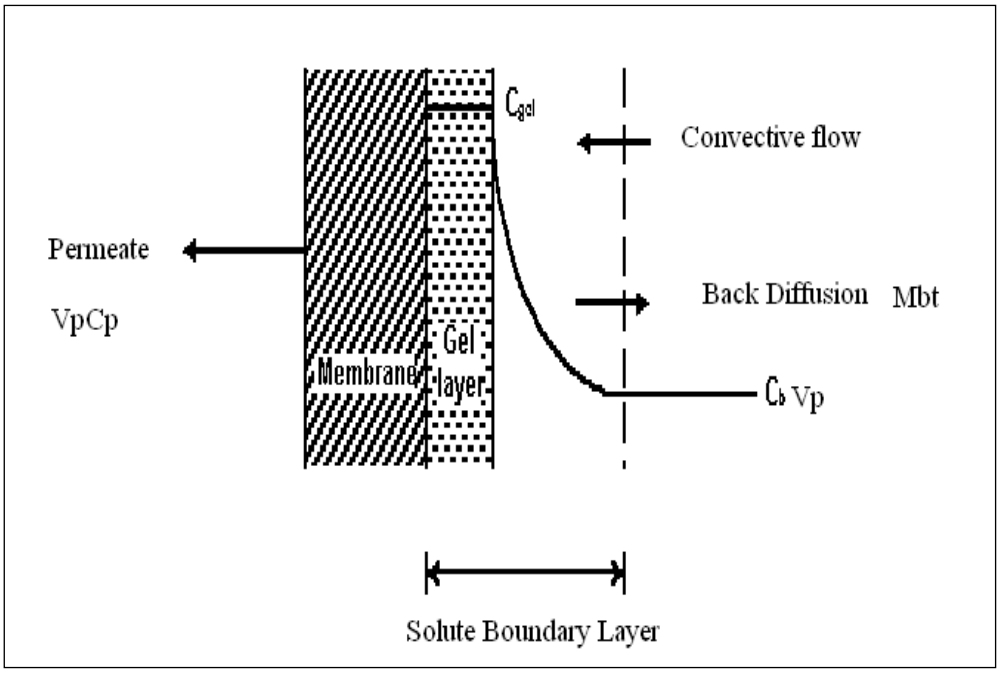

Figure 4.1: Representation of the concentration profile near the membrane interface according to the gel-polarization theory and the solutes overall mass balance.

Using the general mass balance equation to find the overall mass balance over the multiple solutes system in the gel layer at any filtration time.

Input + generation – output – consumption = accumulation (general mass balance equation) (4-2)

The generation and consumption terms refer only to generation of products and consumption of reactants as a result of chemical reaction, in our work there is no chemical reaction then these terms are zero.

At steady state condition and with the assumption that

1. The interaction solute-solute is neglected.
2. Considering the back transport effect, the concentration of each solute can be obtained by mass balance analysis.
3. For diffusion, mass transfer and back transport coefficient each solutes will have its independent value.

Gives the following equation as the following (Ahmed et al., 2006):

$$V_g C_g = (V_p + V_g) C_b - V_p C_p - M_{bt}. \qquad (4\text{-}3)$$

Where C_g is the total concentration of solutes in the gel layer, C_p is the total concentration of solutes in the permeate, C_b is the total concentration of solutes in the bulk V_g is the total volume of gel layer up to time t, M_{bt} is the total back transport mass up to time t and V_p is the total volume of permeate up to time t.

Since we have multiple solutes system we should take the summation of mass balance of each individual solute. Hence, the above equation can be written as the following (Ahmed et al., 2006):

$$V_g \sum_{i=1}^{n} C_{gi} = (V_p + V_g) \sum_{i=1}^{n} C_{bk} - V_p \sum_{i=1}^{n} C_{pi} - \sum_{i=1}^{n} M_{bti} \qquad (4\text{-}4)$$

For i=1,2,3,…….,n.

4.1.2. Transport Phenomena in Membrane

The driving force for membrane filtration treatment is the pressure gradient across the membrane. As a result of this driving force a convective transport of solutes and solvent from the bulk to the membrane surface is obtained. Solvent permeates through the membrane and solutes are retained by the membrane so the solute concentration near that surface will increase.

As a result of the concentration gradient thus generated, solute molecules will diffuse away from the membrane surface. The convective transport to the membrane surface is balanced by the back transport from the membrane surface to the bulk. This back transport is governed by diffusion. In a cross flow membrane filtration process a steady state is reached when the convective transport is equal to the back transport, as a result the permeate flux is constant in time. The back transport is influenced by the flow conditions inside the membrane. The back-transport of for each solute *i* has been assumed to be proportional to both the superficial velocity, v, and the concentration of the solute in the gel layer, C_{gi} (Ahmed et al,2006):

$$\frac{dM_{bti}}{dt} \alpha \ \ vC_{gi} \qquad (4\text{-}5)$$

The above equation can be written as (Bhattacharjee and Datta, 2003) by using the back transport coefficient (K_{bi}) for every solute (i)

$$\frac{dM_{bti}}{dt} = K_{bi} v C_{gi} \qquad (4\text{-}6)$$

After using the initial condition (at $t = 0 \rightarrow M_{bti} = 0$) and integration Eq.(4-4) the following equation will generate (Ahmed et al,2006):

$$M_{bti} = K_{bi} v C_{gi} t \quad \text{for } i = 1,2,3,....., n \qquad (4\text{-}7)$$

In order to find the total permeate (V_p) up to time t, substitute Eq.(4-7) into Eq.(4-4) and rearrange:

$$V_p \sum_{i=1}^{n} (c_{bi} - C_{pi}) = V_g \sum_{i=1}^{n} (C_{gi} - C_{bi}) + vt \sum_{i=1}^{n} K_{bi} C_{pi} \qquad (4\text{-}8)$$

For the gel layer thickness (z) is equal to (V_g / A) where A is the effective are for filtration, rearranging Eq. (4-8) in terms of gel layer to give the following equation (Ahmed et al, 2006)

$$z = \frac{V_p}{A} \frac{\sum_{i=1}^{n} (C_{bi} - C_{pi})}{\sum_{i=1}^{n} (C_{gi} - C_{bi})} - \frac{\sum_{i=1}^{n} K_{bi} C_{gi}}{A \sum_{i=1}^{n} (C_{gi} - C_{bi})} vt. \qquad (4\text{-}9)$$

4.1.3 Polarization Theory

There are three widely accepted models that are used to explain the relationship between permeate flux and operating parameters as described in Chapter 2 (Literature Review). These mechanisms are: 1) the osmotic pressure model, 2) the gel layer model, 3) the resistance model [Jonsson and Tragardh, 1990]. Before explaining these models, a discussion of how fluid flows through membrane pores will be introduced. Fluid flow through porous membranes can be described by the Darcy equation. To yield the expression for the Darcy equation replace the term dX/dx in equation (4-1) by Δp since in the continuous cross-flow system, the driving force is a pressure difference across the membrane.

$$J_v = l_p.\Delta p = \frac{P_m \Delta P_c}{\mu H} \qquad (4\text{-}10)$$

Where D.A is now replaced by the permeability coefficient of the membrane l_p , P_m is the specific permeability, Δp is the pressure difference between the pressure of the bulk side and the permeate side ,μ is the viscosity and H is the membrane thickness. Since the ultrafiltration is a separation process, therefore the solutes are retained on one side of the membrane. Thus, the Darcy equation does not fully describe the flow through the membrane [Jonsson and Tragardh, 1990]. One other problem should be mentioned is that the thickness of the membrane (H) is not constant, the reason is that the pores of the membranes

have increasing diameters. As a result a new term has found to solve this problem, to combine the thickness and the specific permeability to form the hydraulic resistance of the membrane, $R_m = H / P_m$.

4.1.4 Osmotic pressure model:

In order to find the flux decline through the membrane, we should take into account the effect of the concentration polarization at the membrane surface since at the surface the concentration of the solute is larger than the solute on the permeate side (lower solute concentration) as a result the applied hydrostatic pressure on the bulk side has to be larger than the osmotic pressure difference between the bulk and the permeate side. Thus, the osmotic pressure here is important and has to be added to the Darcy's equation (4-7).

$$J_v = l_p(\Delta p - \Delta\pi) = \frac{|\Delta P| - |\Delta\pi|}{\mu R_m} \qquad (4\text{-}11)$$

4.1.5. Resistance model

The reasons for the flux decline is not depend only on the applied pressure and on the osmotic pressure as mentioned previously on both the Darcy's law and the osmotic pressure model equation. In practice, the flux decline also depends on the increased resistance, this can be due to the formation of the gel layer.

Thus, a new term including the gel layer resistance must be incorporated into the Decay's law and the osmotic pressure model equation.

$$J_v = \frac{|\Delta P|}{\mu(R_m + R_g)} \qquad (4\text{-}12)$$

A quantitative description of the flux decline in ultrafiltration involves the following relationship between two of the following three variables which are related by:

$$J_v = \frac{volume}{Membrane.area * time} = \frac{dV_p}{A.dt} = \frac{driving}{vis\cos ity} \frac{force}{* total} \frac{(e.g.\Delta p)}{resis\tan ce} \qquad (4\text{-}13)$$

Therefore, for continuous cross flow ultrafiltraion system using Darcy's law the following equation can be written as (Ahmed et al, 2006).

$$J_v = \frac{1}{A}\frac{dV_p}{dt} = \frac{P_m \Delta P_c}{\mu H} \qquad (4\text{-}14)$$

On other hand, equation (4-12) can be written as

$$J_v = \frac{1}{A}\frac{dV_p}{dt} = \frac{|\Delta P| - |\Delta \pi|}{\mu(R_m + R_g)} \qquad (4\text{-}15)$$

Now, combine Eqs.(4-14) and (4-15) and substitute of the thickness gel layer (z) equation (4-9) and rearrange to get(Ahmed et al., 2006):

$$\frac{1}{J_v} = \frac{\mu R_m}{\Delta P - \Delta \pi} + \frac{\mu}{AP_m(\Delta P - \Delta \pi)} \frac{\sum_{i=1}^{n}(C_{bi} - C_{pi)}}{\sum_{i=1}^{n}(C_{gi} - C_{bi})} V_P - \frac{\mu v}{AP_m(\Delta P - \Delta \pi)} \frac{\sum_{i=1}^{n} K_{bi} C_{gi}}{\sum_{i=1}^{n}(C_{gi} - C_{bi})} t$$

(4-16)

Or

$$\frac{1}{J_v} = a_1 + a_2 V_p - a_3 t \qquad (4\text{-}17)$$

Where

$$a_1 = \frac{\mu R_m}{(\Delta P - \Delta \pi)} \qquad (4\text{-}18)$$

$$a_2 = \frac{\mu}{AP_m(\Delta P - \Delta \pi)} \frac{\sum_{i=1}^{n}(C_{bi} - C_{Pi})}{\sum_{i=1}^{n}(C_{gi} - C_{bi})} \qquad (4\text{-}19)$$

$$a_3 = \frac{\mu v}{AP_m(\Delta P - \Delta \pi)} \frac{\sum_{i=1}^{n} K_{bi} C_{gi}}{\sum_{i=1}^{n}(C_{gi} - C_{bi})} \qquad (4\text{-}20)$$

For i=1,2,3,…….n

By inserting equations (4-17) in the form of first order ordinary differential equation (ODE) gives the following equation of the total permeate volume collected up to time t (Ahmed et al., 2006)

$$\frac{dV_p}{dt} = \frac{A}{a_1 + a_2 V_p - a_3 t} \qquad (4\text{-}21)$$

The usage of Eq (4-17)-(4-20) is to find the permeate volume flux in the multiple solutes system of the continuous cross-flow ultrafiltration .

Considering the overall mass balance over the multiple solutes system of continuous cross-flow ultrafiltration in the gel layer to find the concentrations of each solute in the permeate, the mass balance can be written as (Ahmed et al., 2006).

$$V_g C_{gi} = (V_p + V_g) C_{bi} - V_p C_{pi} - M_{bti} \qquad (4\text{-}22)$$

Now, in order to find the total permeate volume up to time t a substitution of Eq.(4-7) into (4-21) gives (Ahmed et al., 2006)

$$V_p (C_{bi} - C_{pi}) = Az(C_{gi} - C_{bi}) + K_{bi} v C_{gi} t \qquad (4\text{-}23)$$

Then, a differentiate of Eq. (4-23) with respect to time t , can be written as (Ahmed et al., 2006)

$$(C_{bi} - C_{pi}) J_v = \frac{dz}{dt}(C_{gi} - C_{bi}) + \frac{K_{bi} v C_{gi}}{A} \qquad (4\text{-}24)$$

In a steady state situation, which is reached after some time, the amount of solute diffuses back to the bulk of the solution, is equal to the amount of solutes transported towards the membrane. Thus, the gel layer thickness will remain constant and the solutes deposition rate at the membrane surface can be written as (Ahmed et al., 2006).

$$\frac{dz}{dt} = 0 \qquad (4\text{-}25)$$

Now in order to find the concentration of solute (i) in the permeate C_{pi} of the multiple solutes system of continuous cross-flow ultrafiltration, inserting of Eq.(4-25) into Eq.(4-24) will give the following expression for C_{pi} (Ahmed et al,2006)

$$C_{pi} = C_{bi} - \frac{K_{bi} v C_{gi}}{A J_{v,ss}} \qquad \text{for i=1,2,3,……,n.} \qquad (4\text{-}26)$$

Where $J_{v,ss}$ is the volume flux of permeate at the steady-state condition (Ahmed et al, 2006).

However, the concentration of solute i in the gel layer, C_{gi} should be known to calculate the concentration of solute i in the permeate (C_{pi}).

4.1.6 Gel polarization model

As mentioned earlier on chapter (2) , Bhattacharjee and Datta (2003) derived the gel polarization model that describes the permeate flux .The model equation for the film theory coupled with a boundary layer condition $C_m = C_g$ for all t , Eq.(2.4.) changed into (Ahmed et al,2006)

$$\frac{(C_{gi} - C_{pi})}{(C_{bi} - C_{pi})} = \exp(\frac{J_{v,ss}}{k_i}) \qquad (4\text{-}27)$$

Where k is the mass transfer coefficient. The gel polarization model now can be used to find the concentration of solute i in the gel layer.

Chemical Oxygen Demand

In (Ahmed et al, 2006) work, the efficiency of ultrafiltration treatment process was measured by using the Chemical oxygen demand (COD) method. This method is used to measure the amount of pollution in a wastewater sample by measuring the oxygen requirement in that sample that is susceptible to oxidation by strong chemical oxidant also it used assessing treatment ultrafiltration performance. The higher the chemical oxygen demand, the higher the amount of pollution in the test sample.

A linear correlation is used in this work to relate the concentration of all solutes in the system with the chemical oxygen demand (COD)

$$C_{COD} = \sum_{i=1}^{n} b_i C_i \qquad \text{for } i = 1.2.3\ldots\ldots\ldots\ldots\ldots n. \qquad (4\text{-}28)$$

where C_i is the concentration of solute i in the system and b_i is the dimensionless coefficients related to the concentration of all solutes and it was

found by using the Levebenberg-Marquardt method. The obtained correlations values were ($b_1 = 0.3535$, $b_2 = 4.9279$ and b_3=0.5595) .

The final form of equation (4-28) will be as the following (Ahmed et al, 2006)

$$COD_{calculated} = 0.3535C_{p,carbohydrate} + 4.9279C_{p,protein} + 0.5595C_{p,nitrogen} \quad (4\text{-}29)$$

4.1.7 Parameter estimation method

Most of the previous works regarding the development of membrane ultrafiltration model were based on mass balance analysis coupled with the filtration theory. For the membrane parameter, which are $(R_m, \Delta\pi, P_m, \mu, K_{bi}, k_i)$ **,** were obtained from the experimental data of Ahmed et al, 2006 using the parameter estimation method.

R_m is the resistance of the membrane which can be evaluated directly from the slope of the J_w (pure water flux) versus ΔP as described by (Ahmed et al, 2006).

$$R_m = \frac{\Delta P}{J_w} \quad (4\text{-}30)$$

To obtain the mass transfer coefficient (k_i) of each solute from the experimental data the velocity variation method was used (Ahmed et al., 2006).

4.1.8 The velocity variation method

A method based on the variation on observed rejection when cross-flow velocities are changed.

By a linearization of Eq.(4-26) using the observed rejection term($R_{oi} = 1 - \frac{C_{pi}}{C_{bi}}$) and the true (real) rejection term ($R_i = 1 - \frac{C_{pi}}{C_{gi}}$), the following relation can be derived

$$\ln(\frac{1}{R_{oi}} - 1) = \frac{1}{q}(\frac{J_{v,ss}}{v^{\eta}}) + \ln(\frac{1}{R_i} - 1) \qquad (4\text{-}31)$$

Where R_i is the real (true) rejection (retention) of solute i and R_{oi} is the observed rejection (retention) of solute i.

The difference between both the true rejection and the observed rejection is very important to understand.

The observed rejection tells what rejection the whole system can be perform while the true rejection what rejection the membrane can be able to perform.

By plotting the experimental values of $\ln(\frac{1}{R_{oi}} - 1)$ as a function of $(\frac{J_{v,ss}}{v^{\eta}})$, the constant q and η can be defined graphically from the best linear fit .Since

generally the mass transfer coefficient (k) value can be calculated from Sherwood relations of the form used by several researchers (Tu.et al, 2001),

$$Sh = kd_h / D = p\,\mathrm{Re}^q\, Sc^r \qquad (4\text{-}32)$$

Where:

d_h is the hydraulic diameter of the system.

D is the diffusion coefficient .

Re is the Reynolds number and is equal to ($\frac{\rho v d_h}{\eta}$).

Sc is the Schmidt number and is equal to $(\frac{\eta}{\rho D})$.

p, q and r are adjustable parameters.

These correlations establish the dependence of the mass transfer coefficient on the fluid dynamics of the system.

The Sherwood relations for k its always depend on the superficial velocity of the type

$k_i = qv^{\eta}$.

For each solute the back transport coefficient (K_{bi}) for each solute can be determine by using equation (4-26). By plotting C_{pi} as a function of ($\frac{vC_{gi}}{AJ_{v,ss}}$) the slope of the plot will represent the K_{bi} value. In (Ahmed et al, 2006) work, the experimental data on the ultrafiltration was obtained by measuring the change at various concentrations and pressures at steady state and constant feed flowrate.

Levenberg–Marquardt algorithm coupled with the Gauss-Newton algorithm to facilitate the parameter estimation, which will be used to simulation purpose. These two models were used to estimate the parameters of a_1 a_2 , a_3 in Eq.(4-17) by collecting several experimental with V_p and t as independent variables and $1/J_v$ as dependent variable and these data were fitted into Eq (4-17) . After the parameters a_1 a_2 , a_3 values were found Eqs. (4-18)- (4-20) can be used now to find the unknown parameters ($\Delta\pi, P_m$).

The viscosity of the bulk (μ) can be found experimentally.

Model Numerical Solution and PredictionBy knowing the membrane parameters $(R_m, \Delta\pi, P_m, \mu, K_{bi}, k_i)$ from the experimental data using the

parameter estimation method and the operating parameters $(\Delta P, v, C_b, C_{bi})$ equations (4-17) and (4-20) have been solved simultaneously by using the software package of matlab 7.0. For Eq.(4-21) it has been solved by implementing implicit Runge –kutta method.

The above model formulation represents the mass balance equations for the continuous cross-flow ultrafiltration system in rather general form coupled with the three different filtration theory that have been used to develop a time-dependent mathematical model to predict the performance of an ultrafiltration process by imposing a series of restrictions and assumptions.

Now as the new model (development model), which takes into account the three important mechanisms (i.e. gel-boundary layer controlled model, osmotic pressure controlled model as well as gel-layer resistance model that were described in detail in Chapter 2 and implicitly in the current Chapter 4.) was proposed here. Let us investigate separately the capability of each three models in predicting the complete flux behavior.

Further, in the following sections the flux data were analyzed by three conventional models: osmotic pressure model, gel polarization model and gel-layer resistance model since these three models are more theoretical meaning than the others, and they can predict the flux for a wide range of operating transmembrane pressure.

In the present work, for every model the model equations were incorporated in EXCEL ^{TM} for output of results. The output results of the model were compared with experimental data from Ahmad et al., (2006) as seen in the following Figures (4.2-4.12). The comparison between the fluxes predicted by the osmotic-pressure model, gel polarization model and the resistance model was discussed in terms of the ability of each model to predict well the experimental data that were described previously in Chapter 3.

Let us start on the following section (section 4.2.1) with simplest model of ultrafiltration the osmotic pressure model.

4.2 Simple models comparison with the development model

4.2.1 Flux prediction by the Osmotic pressure model

The osmotic pressure is the sole controlling mechanism for solutes that do not form gel and it has received more and more attention recently. As it was mentioned previously the aim of this work is to it to investigate whether this model is capable of predicting the complete flux behavior or no.

By getting back to Chapter (2), Kedem and Katchalsky gave the equation for the osmotic pressure model Eq.(2-6).

In order to calculate the osmotic pressure for the solution we can use the Van't Hoff equation, it is based on the virial coefficients as given

$$\Delta\pi = \frac{RT}{M}\left(C_b + B_2 C_b^2 + B_3 C_b^3\right) \qquad (4\text{-}33)$$

Where R is the gas constant, T the absolute temperature, M the molar mass , C_b the bulk concentration and B_1, B_2 and B_3 are the virial coefficients.

Model equations (2-6) and (4-33) were incorporated in EXCEL ^{TM} for output of results. The output results of "Osmotic pressure" model were compared with experimental data from Ahmad et al., (2006).

The permeate flux decline as predicted by the osmotic pressure model are shown in the following three figures, where the flux decline is plotted against the filtration time with the increasing transmembrane pressure, feed flowrate and bulk concentration as seen in fig (4.2), fig (4.3) and fig (4.4) respectively.

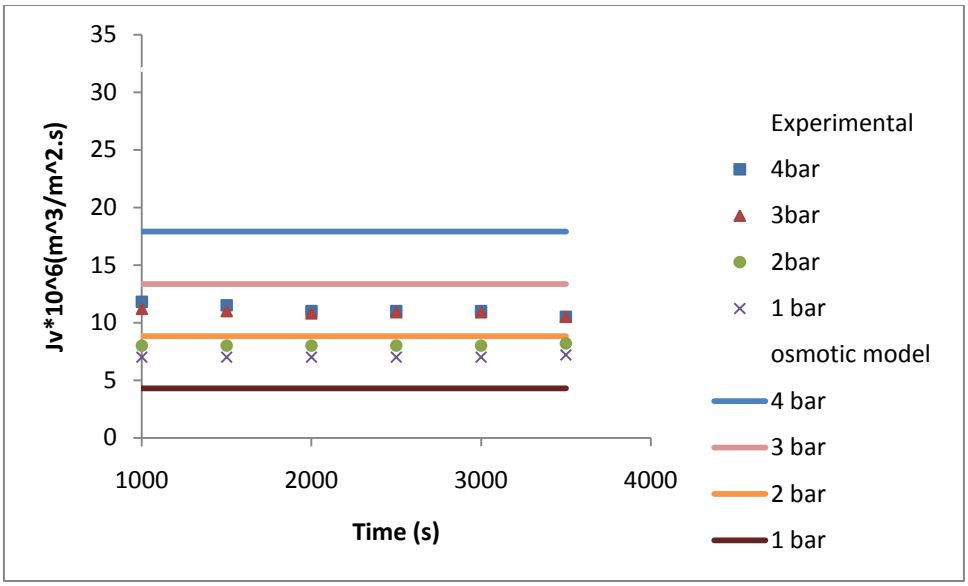

Figure(4.2): Comparison of the "osmotic pressure " model predictions with experimental data (Volume flux of permeate against filtration time at different transmembrane pressure and constant feed flowrate = 4 m3/hr and constant bulk concentration =5720 mg/l) from Ahmad et al., (2006).

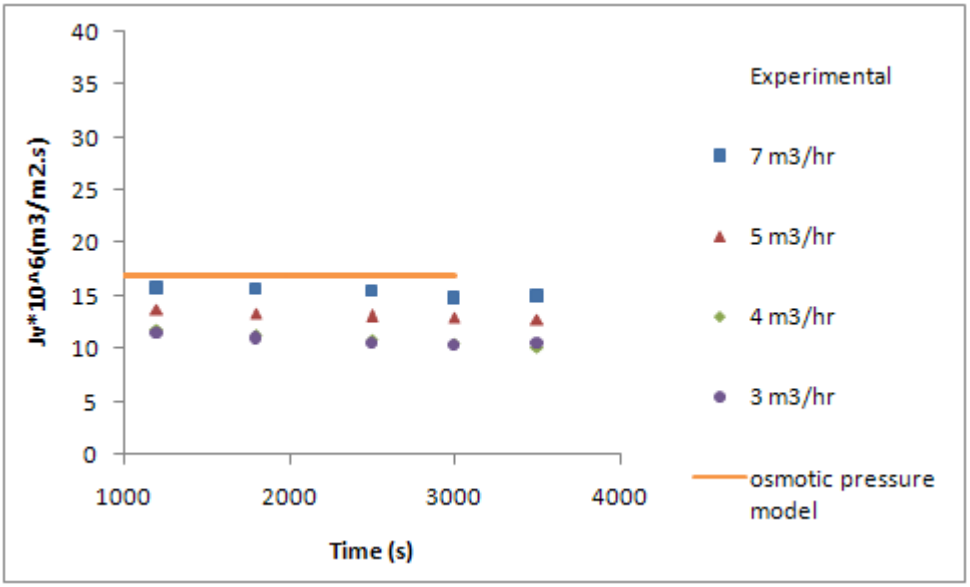

Figure(4.3): Comparison of the "osmotic pressure " model predictions with experimental data (Volume flux of permeate against filtration time at different flowrate and constant transmembrane pressure= 4 bar and constant bulk concentration =5720 mg/l) from Ahmad et al., (2006).

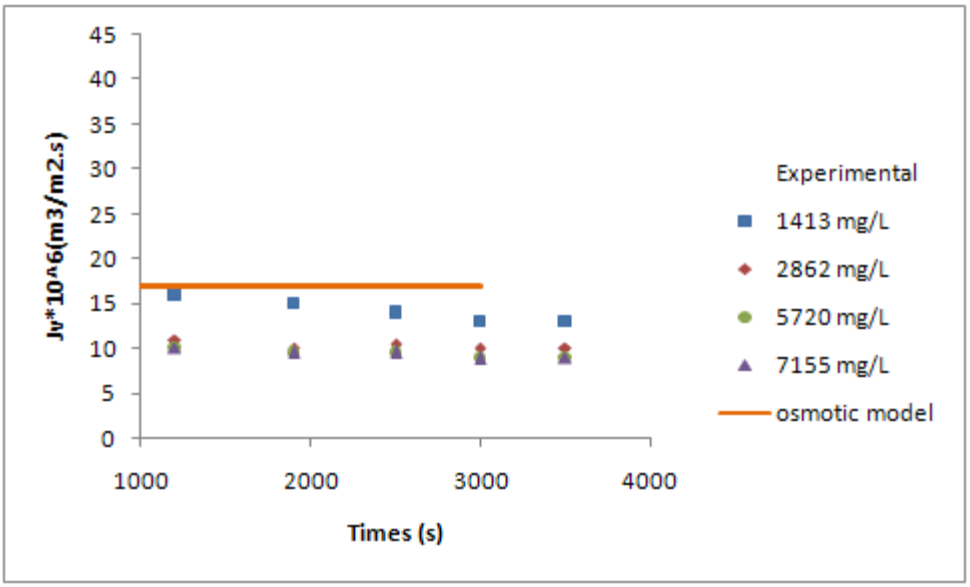

Figure (4.4): Comparison of the "osmotic pressure " model predictions with experimental data (Volume flux of permeate against filtration time at different bulk concentration and constant feed flowrate = 4 m3/hr and constant transmembrane pressure= 4 bar) from Ahmad et al., (2006).

The predicted flux of the model was compared with experimental data. The solid lines correspond to the values calculated by the model while the symbols correspond to the experimental results on the permeate flux versus time. It can be clearly observed that the osmotic pressure model didn't show the rapid initial flux decline that corresponds to the fouling of the membrane and the gel layer resistance. In other words, the predicted permeate flux remained constant from the beginning.

There is no doubt that the failure of the osmotic model in describing the experimental data at the given reported conditions is due to the fact that the model does not takes into account the resistance due to the cake formation and

the concentration polarization which are the main fouling mechanism considered in this work. For example, although the osmotic pressure model takes into account the effect of bulk concentration on the osmotic pressure of the medium as given by equation (4-33), the model doesn't seem to predict the effect of increasing bulk concentration on the flux decline as seen in Figure (4.4). Where Figure (4.4) shows that prediction by the osmotic pressure model at four different bulk concentrations are so close to each other that they seem to be one line. This is because the effect of bulk concentration on the osmotic pressure only is negligible compared to the effect of bulk concentration on other mechanisms (i.e. concentration polarization and cake formation), which are not taken into account by the osmotic pressure model.

Therefore, we can conclude that the model does not describe experimental data and it over predicts the actual volume flux of permeate. By plotting the initial experimental values of flux versus the initial values of predicted flux by the model at different transmembrane pressures as given in (Figure 4.5), we can see that the model seems to be somehow able to describe only the initial stage of flux decline at different transmembrane pressures.

Thus, if our goal is to accurately predict the flux decline during the ultrafiltration process, the present model has to be extended to include concentration polarization and cake formation as will be presented in the following sections.

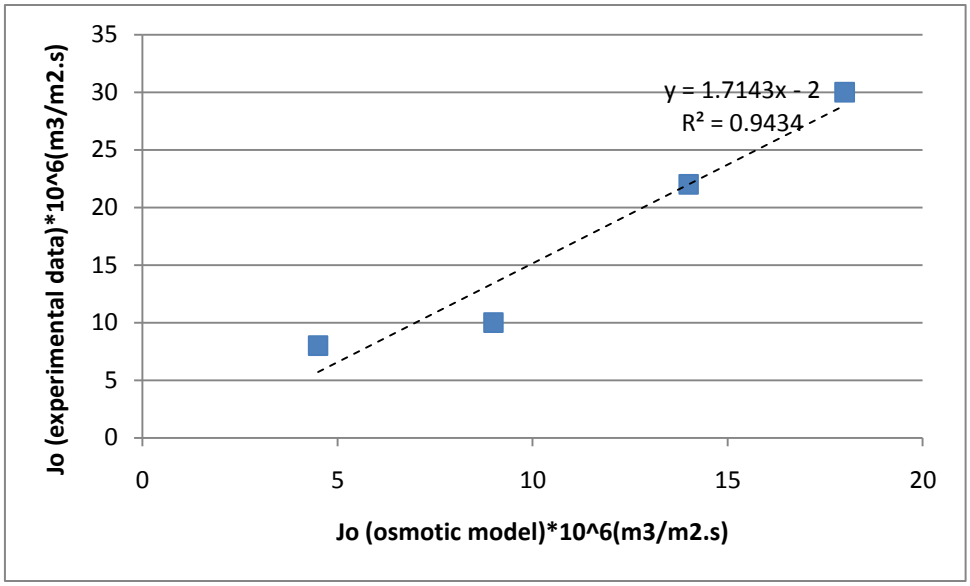

Figure (4.5): Experimental flux of permeate against osmotic model flux at four different pressures .

4.2.2 Flux prediction by the Gel-layer Resistance model

It is also possible to describe the flux decline on the basis of the gel-layer resistance phenomenon, and the permeate flux is then written using the hydraulic resistance of the boundary layer R_H . The hydraulic resistance, is equal to the summation of the membrane resistance R_m, and the gel layer resistance, R_g . By neglecting the osmotic pressure term in Eq. (2-6) and based on Darcy's Law the permeate flux, J_v may be expressed as Eqn. (2-13).

The gel-layer resistance Rg also manifests temporal variation until steady state is reached. The progressive accumulation of solute on the membrane (gel-layer formation) is due to the difference between the net solute transport from the

bulk solution to the membrane and solute back-diffusion from the membrane to the bulk solution and is represented as (Tu.et al, 2001):

$$\frac{dR_g}{dt} = \frac{\varepsilon}{\rho_g} C_b J_v - \frac{\varepsilon k}{\rho_g} C_b In \frac{C_g}{C_b} \qquad (4\text{-}34)$$

$$R_g = \varepsilon L_g \qquad (4\text{-}35)$$

Where ε is the resistance per unit of the gel-layer thickness, L_g and ρ_g represent density and rhickness of the gel-layer respectively.

The mass transfer coefficient k can be calculated from Sherwood correlations Eq. (4-32).

The comparison of the resistance model prediction of flux decline with the experiment result is shown in fig (4.6), fig(4.7) and fig (4.8).

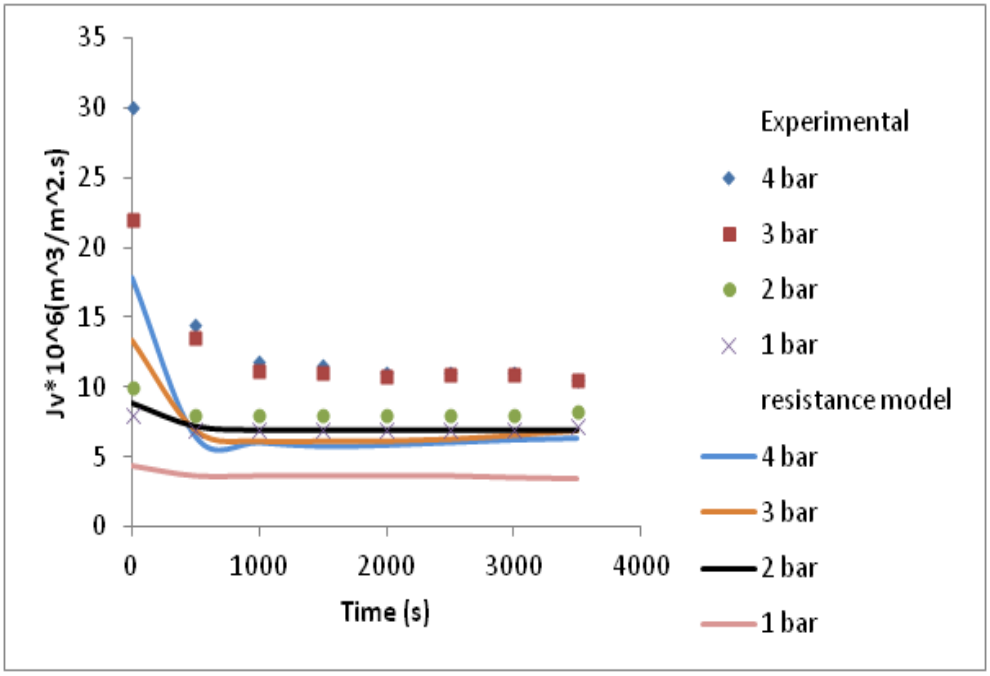

Figure (4.6): Comparison of the "gel-layer resistance" model predictions with experimental data (Volume flux of permeate against filtration time at different transmembrane pressure and constant feed flowrate = 4 m3/hr and constant bulk concentration =5720 mg/l) from Ahmad et al., (2006).

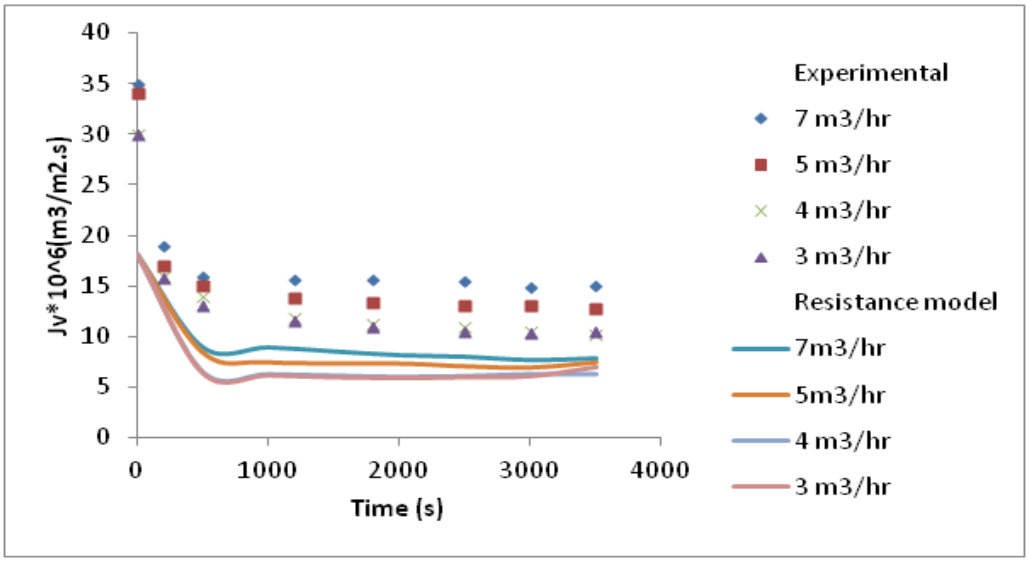

Figure (4.7): Comparison of the "gel-layer resistance" model predictions with experimental data (Volume flux of permeate against filtration time at different feed flowrate and constant transmembrane pressure= 4 bar and constant bulk concentration =5720 mg/l) from Ahmad et al., (2006).

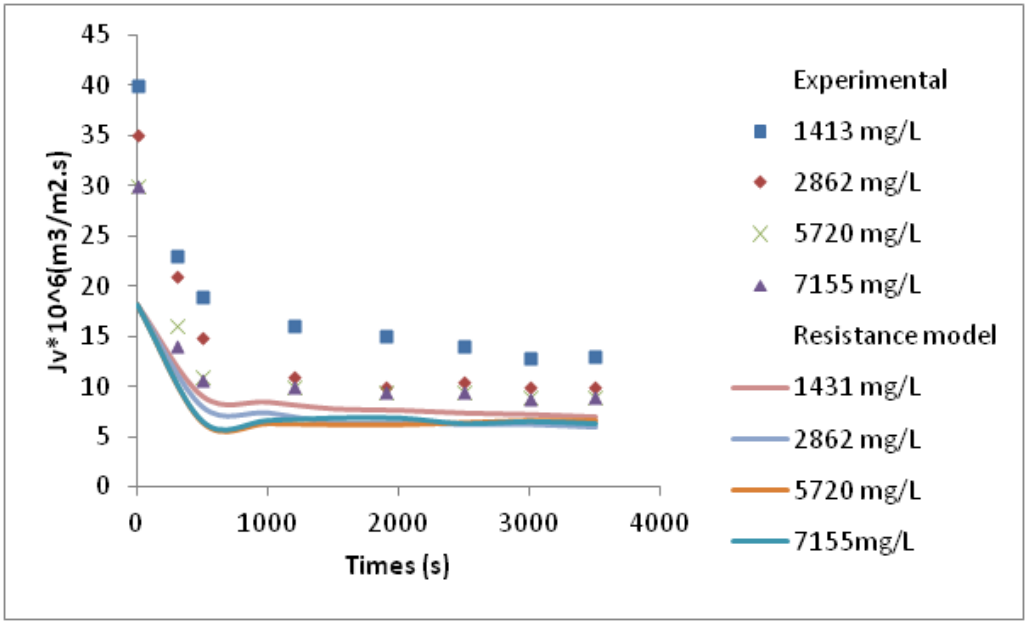

Figure (4.8): Comparison of the "gel-layer resistance" model predictions with experimental data (Volume flux of permeate against filtration time at different bulk concentration and constant feed flowrate = 4 m3/hr and constant transmembrane pressure= 4 bar) from Ahmad et al., (2006).

Experimental and predicted results from the resistance model were compared. The solid lines represent the gel-layer resistance model prediction while the symbols lines represent the experimentally obtained flux values. The figures provide a better picture of the resistance model prediction. It can be observed that permeate flux estimated by the model is slightly more close to the experimental results although the predicted results are slightly lower than experimental results.

Moreover, the shape of the curve that corresponds to the predicted permeate flux is similar to that experimentally obtained. Nevertheless, for short time scales the model predicts less fouling than that experimentally observed.

While the gel-layer resistance model qualitatively predicts the correct trends it, quantitatively fail to predict the actual flux decline.

However, the resistance model describes the experimental data of Ahmad et al., (2006) system much better than the osmotic pressure in Figures 4.2, 4.3 and 4.4. This is due to the fact that the permeate flux reached a constant value following an initial decrease since this model have a value for Rg (fouling layer resistance) and that value increases with time due to fouling resulting in lower J with time.

We can conclude that, the " gel-layer resistance model " is slightly more successful in describing the effect of operating condition on both the early and later stages of flux decline curve (i.e. during the whole operating time) and the model was able to predict the flux decline qualitatively (the general trend) but not quantitatively.

The gel-layer resistance model can result in a closer agreement with the experimental data than the osmotic model.

4.2.3 Flux prediction by the Gel polarization model

The gel polarization model is base on a mass balance of solute in the mass transfer boundary layer. At the steady state condition the convective solute transport toward the membrane is equal to the sum of the solute flux through the membrane and the diffusive back transport of the solute.

As mentioned earlier on section (4.3.6). The model equation for the film theory coupled with a boundary layer condition $C_m = C_g$ for all t, give the gel model equation, Eq. (4-27) (Ahmed et al, 2006).

The model all use the film theory to describe the concentration polarization phenomena is based on the assumption that the concentration of solute on the membrane cannot exceed a fixed (*Cg*) value. After ultrafiltration process start, first a polarization layer is formed. Once gel concentration has been reached, an increase of the applied pressure will then only result in an increased of the gel layer thickness but not in an increase in flux.

The comparison of the gel polarization model prediction of flux decline with the experiment result is shown in fig (4.9) and, fig (4.10).

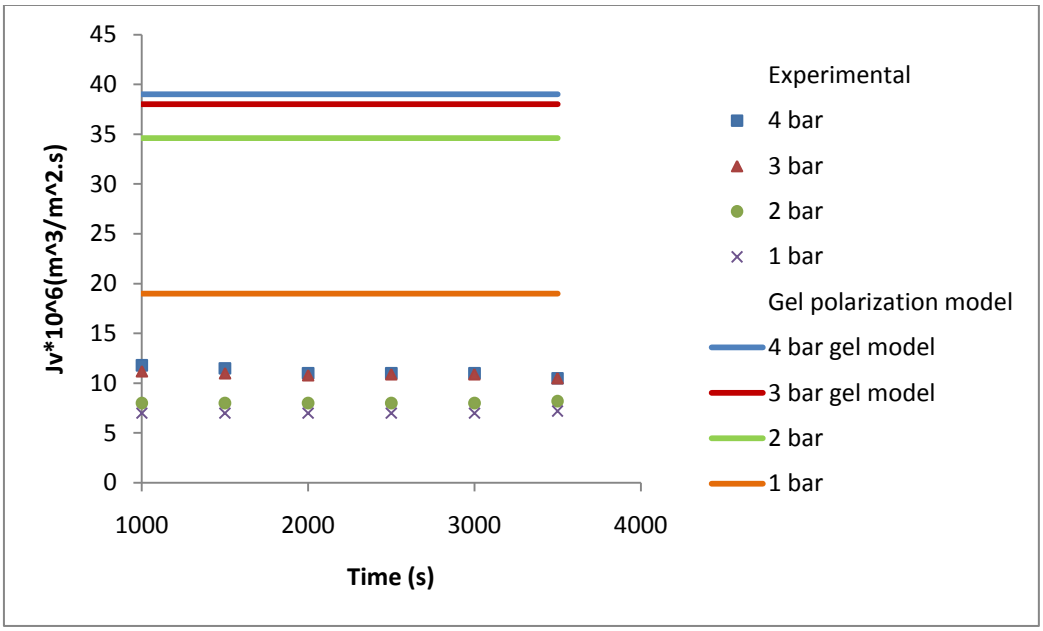

Figure(4.9): Comparison of the "gel polarization " model predictions with experimental data (Volume flux of permeate against filtration time at different transmembrane pressure and constant feed flowrate = 4 m3/hr and constant bulk concentration =5720 mg/l) from Ahmad et al., (2006) .

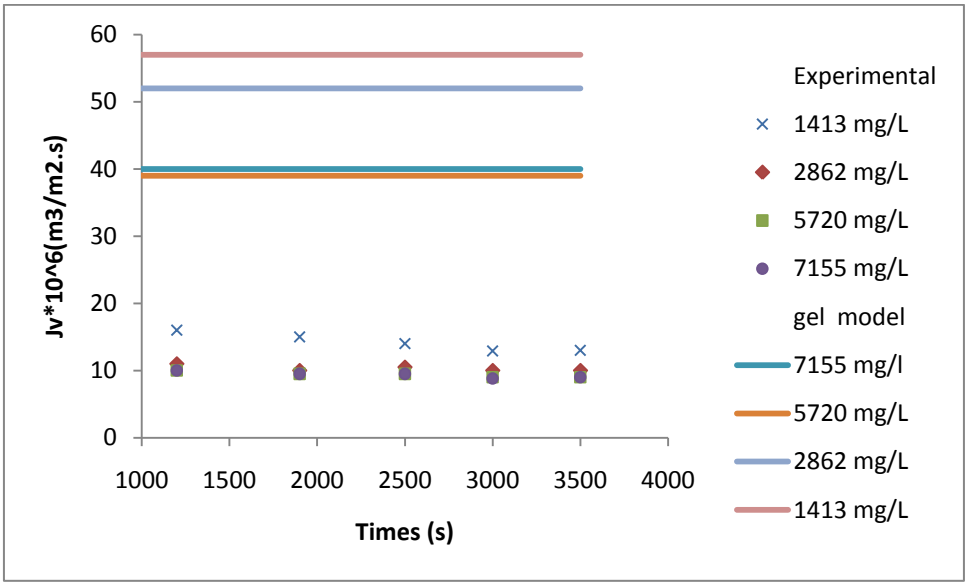

Figure (4.10): Comparison of the "gel polarization" model predictions with experimental data (Volume flux of permeate against filtration time at different bulk concentration and constant transmembrane pressure= 4 bar and constant bulk concentration =5720 mg/l) from Ahmad et al., (2006).

The solid lines correspond to the values calculated by the model while the symbols correspond to the experimental results on the permeate flux versus time. It can be observed that the gel model can't be used solely to explain the experimental permeate flux as seen in figures (4.9) and (4.10).

Furthermore, the gel polarization model doesn't predict the rapid initial flux decline. This can be attributed to the fact that the gel-layer equation (4-27) describes the flux of permeate at steady state only. Also this may be due to the fact that although the model considers the gel boundary layer concentration as a model parameter, the model is not very sensitive to its variation.

However, the model is not sufficient to describe the dynamics of the early stages while it is more likely to predominate in the later stages. This is due to the fact that the model considers concentration polarization as the main mechanism responsible for the permeate flux decline in the early stages while it is actually the formation of the cake layer can be formed in the very early beginnings of ultrafiltration.

We can conclude that the model describes qualitatively the effect of pressure on the flux at steady state. However it does not describe accurately the initial flux of permeate. The worst permeate flux predictions are obtained for short time scales. This can be due to the fact that steady-state conditions were considered to estimate the gel layer concentration. For short time scales, the

model predicts less fouling than that experimentally observed for the experimental conditions tested.

As a result the gel layer polarization model doesn't result in a closer agreement with the experimental data than the resistance model. Also by plotting the initial experimental values of flux versus the initial values of predicted flux by the model as given in Figure 4.11, we can see that there is a lack of linear correlation between the experimental values and the predicted ones. This indicates that the gel layer polarization model does not also describe the early stages of flux decline during the ultrafiltration process. However, if we plot the steady-state experimental values of flux versus the steady-state values predicted by the gel resistance model as given in Figure 4.12, we can see a strong linear correlation. Such a strong linear correlation between the experimental permeates flux at steady-state versus the predicted values by the gel layer polarization -model seems to indicate that the flux-decline is controlled by the gel layer polarization mechanism at later stages.

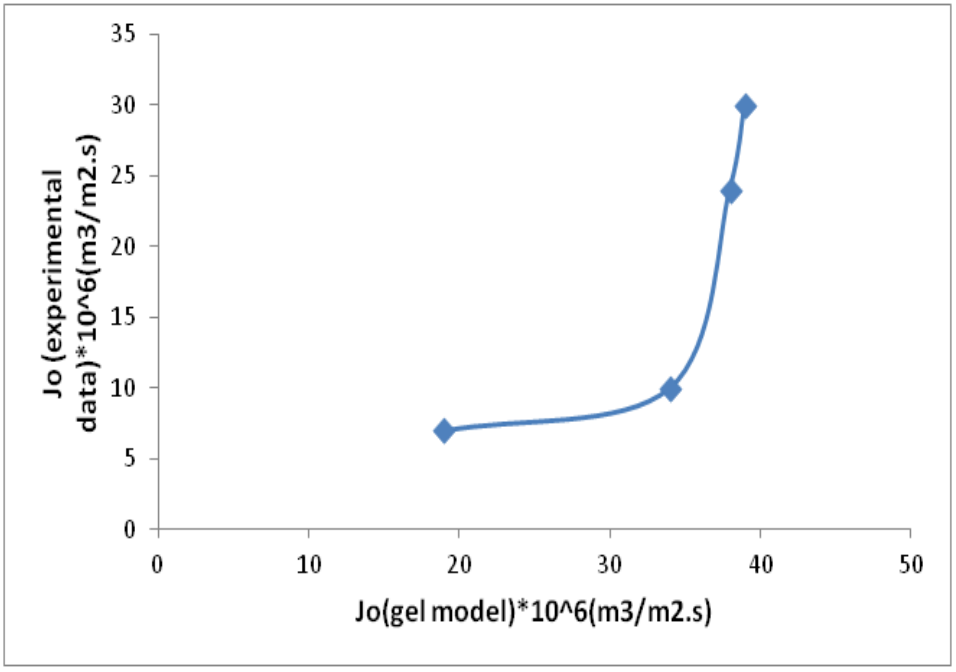

Figure (4.11): Experimental flux of permeate against the flux predicted by the gel layer polarization model.

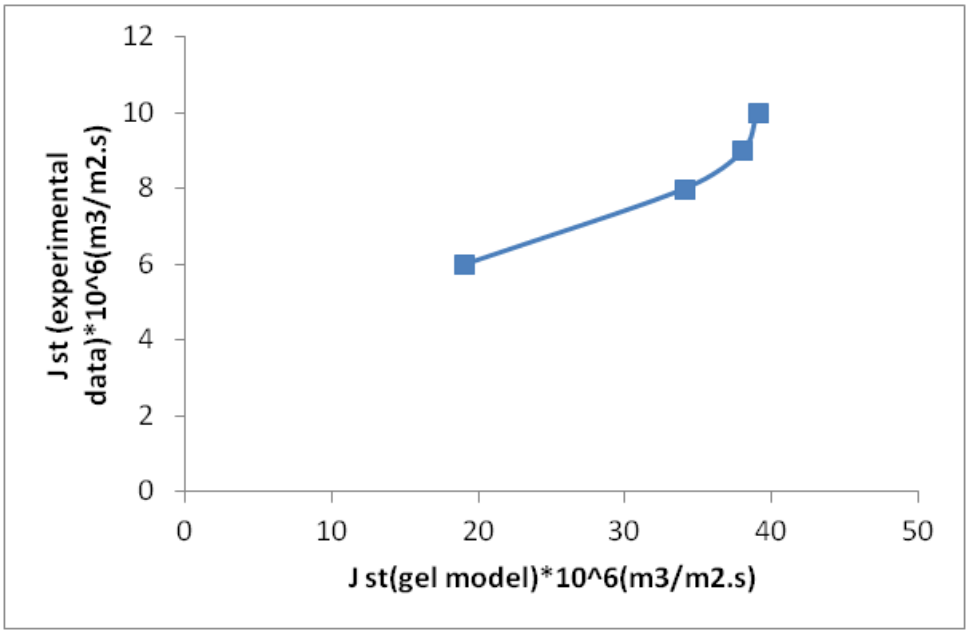

Figure (4.12): Experimental flux of permeate at steady state against the flux predicted by the gel layer polarization model at steady state.

4.3. Comparison between the simulation results of Ahmed et al., 2006) model and the experimental data

4.3.1. Comparison between the simulation results of Ahmed et al., 2006 model and the experimental data of the Volume flux of permeate.

The data estimated by the model were compared with the experimental results in Fig (4.13-4.14 and 4.15), where the total flux of permeate collected against time for the various operating conditions (transmembrane, pressure, feed flowrate and bulk concentration).

1. Different transmembranr pressure

Pressure is the main driving force in the membrane separation process. The effects of the transmembrane pressure on permeate was thus studied. The variation in the volume flux of permeate with time at different transmembrane pressure (varying from 1 bat to 4 bar) are shown in Figure (4.13). The feed flowrate, the superficial velocity and the bulk concentration were kept constant at 4 m3/hr, 2 m/s and 5720 mg/L respectively. For each solute in the bulk the concentration was constant (carbohydrate constituents 3015 mg/L ,crude protein 2675 mg/L and for ammonical nitrogen the concentration kept constant at 34 mg/L).

The solid lines correspond to the values calculated by the model while the symbols correspond to the experimental results on the permeate flux versus

time. The permeate flux estimated by the model is very similar to the experimental result. The flux of the permeate decreases with the time reached a steady state value following an initial decrease caused by the fouling of the membrane .At the same time , with the increase in transmembrane pressure from (1 to 4 bar) an increase in the volume flux of permeate was observed until a critical value of transmembrane pressure (3 bar) achieved. The flux first increase with the increasing transmembrane pressure and finally becomes constant leading to steady state flux vale and any further increase in the pressure will not increase the steady state flux and the membrane system will operate on it is critical flux value since when limiting flux is attained and the pressure increase will not have a positive effect on permeate flux.

Critical flux is the flux at which colloidal deposition takes place below the critical flux value, the flux is directly proportional to transmembranepressure (TMP). However, flux could become independent of pressure if the pressure is beyond a critical point due to concentration polarization and membrane fouling.

These results were also observed by Huang and Morrisey (1998) and Lin et al. (1995). According to the authors, the permeate flux cannot be further increased after gel polarization occurs, and it may eventually decrease with further transmembrane pressure increase due to compaction of the gel layer.

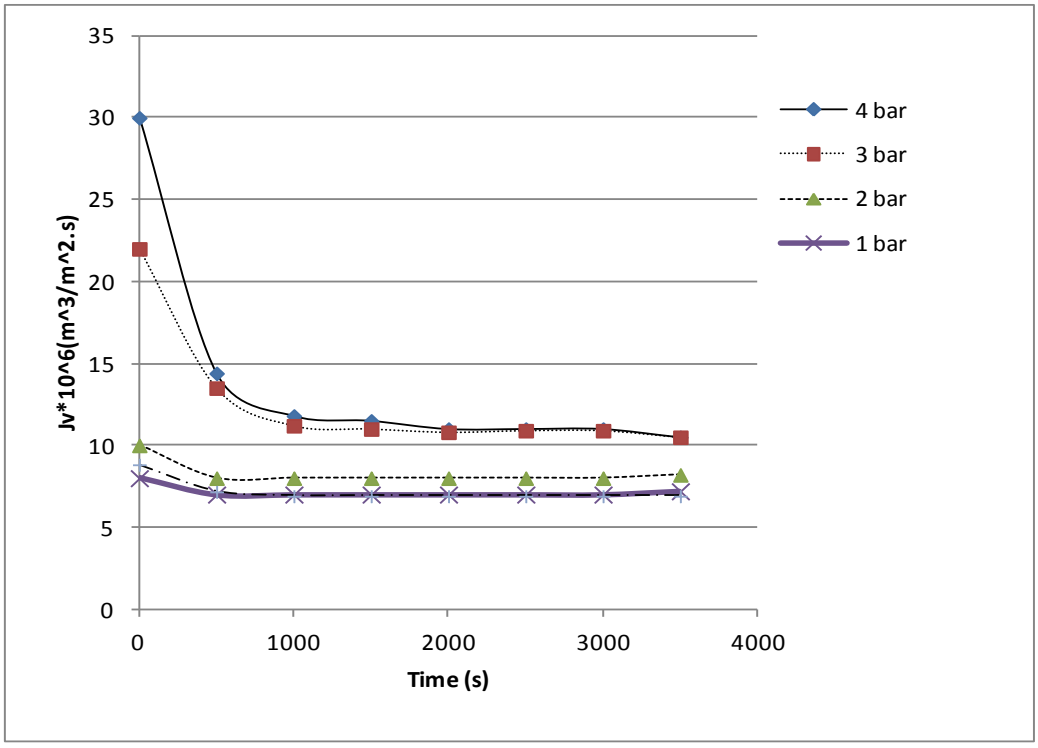

Figure (4.13): Volume flux of permeate against filtration time at different transmembranr pressure.

2. Different feed flowrate

Feed flow rate is another major parameter affecting the membrane performance. Model predictions were compared with the experimental data for constant transmembrane pressure of (4 bar) , constant bulk concentration of (5720 mg/L) and at four different feed flow rate varying from (3 to 7 m3/hr). Again the simulated results are able to represent the experimental data. As shown in fig (4.14) the volume flux of permeate increases with the increase of

feed flowrate (cross-flow velocity)that include the initial and the steady state flux, that for two important reasons:

First the concentration polarization (accumulation of deposited solutes on the membrane surface) decreases with the increase of the flow velocity because of the higher back transport of the rejected solutes into the bulk and this will lead to the second reason that the membrane fouling resistance decreases with the increase of flow velocity since a thinner gel layer was formed .

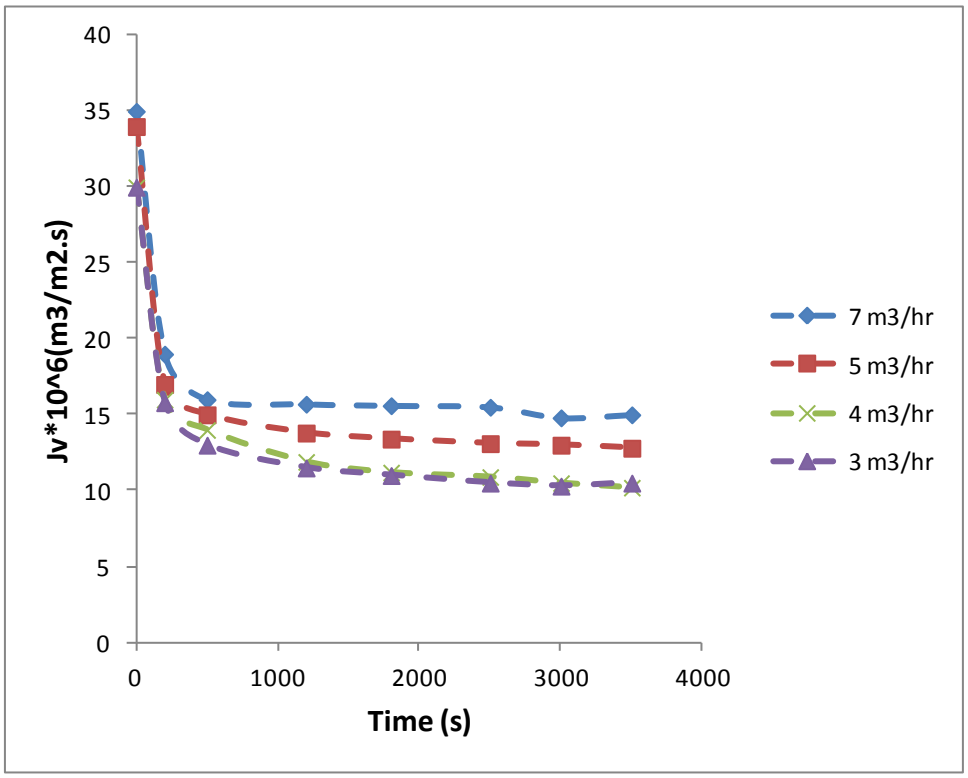

Figure (4.14): Volume flux of permeate against filtration time at different feed flowrate.

3. Different bulk concentration

Another major parameter that affects the membrane performance is the bulk concentration. Figure (4.15) shows the variation in the volume flux of permeate with time when the transmembrane pressure kept constant at 4 bar and the feed flow rate flow was 4 m3/hr under different bulk concentration varying from 1431 to 7155 mg/L. It can be clearly observed from the figure that the volume flux of permeate decrease with the increase of the bulk concentration due to the increase of the resistance due to the greater accumulation of the deposited solutes on the membrane surface with increase of the bulk concentration .

As the bulk concentration increases, the solutes rejection increases. Solutes are retained by the membrane to build up a boundary layer on the membrane surface which accumulates the solutes and reduces the permeate flux. The simulation results show a good agreement with the experimental data as before.

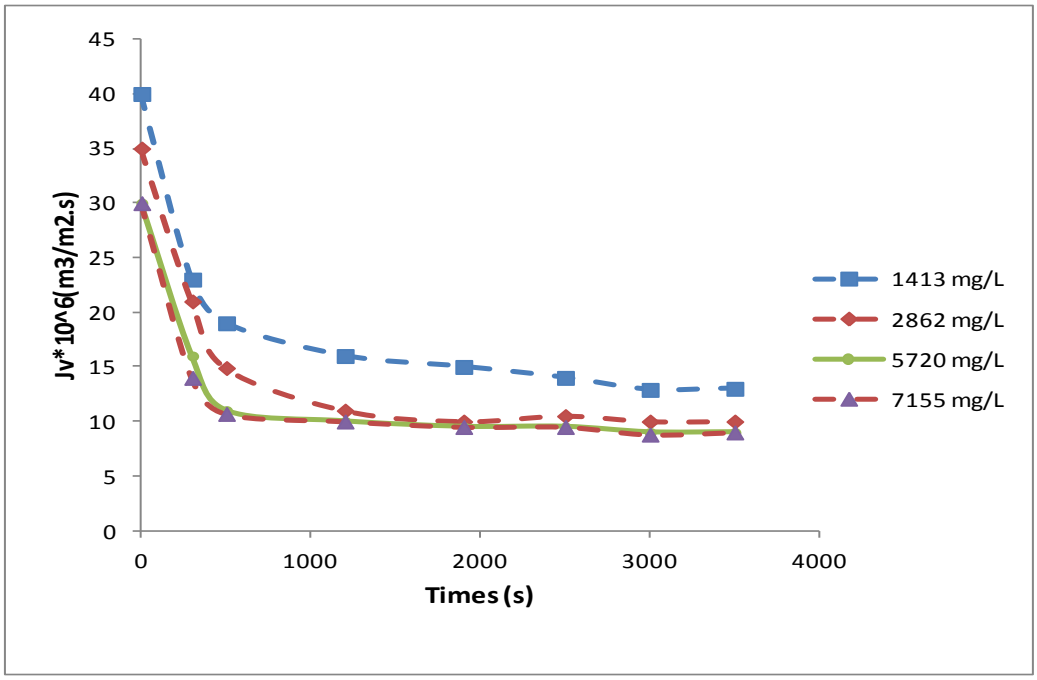

Figure (4.15): Volume flux of permeate against filtration time at different bulk concentration.

4.3.2. Comparison between the simulation results of (Ahmed et al., 2006) model and the experimental data of the total volume of permeate

Now, consider the effect of the same operating conditions (transmembrane, pressure, feed flow rate and bulk concentration) on the total volume of permeate collected against time, three graphs were generated Figs (4.16-4.17 and 4.18). The shape of the curve that corresponds to the total

volume of the permeate is similar to the volume flux of permeate obtained in fig (4.13-4.14 and 4.15).

1. Different transmembrane pressure.

Figure (4.16) presents the permeate flux at different transmembrane pressure varying from (1 to 4 bar) while the feed flow rate was maintained constant at 4 m3/hr and the bulk concentration kept constant at 5720 mg/L. It is noticeable in Figure (4.16) that when increasing transmembrane pressure from 3 bar to 7bar, the permeate flux increases. This is due to the fact that at higher transmembrane pressure the rate of deposition and fouling would be higher and this will lead to compress the rejected solute into a denser fouling layer with increased fouling resistance.

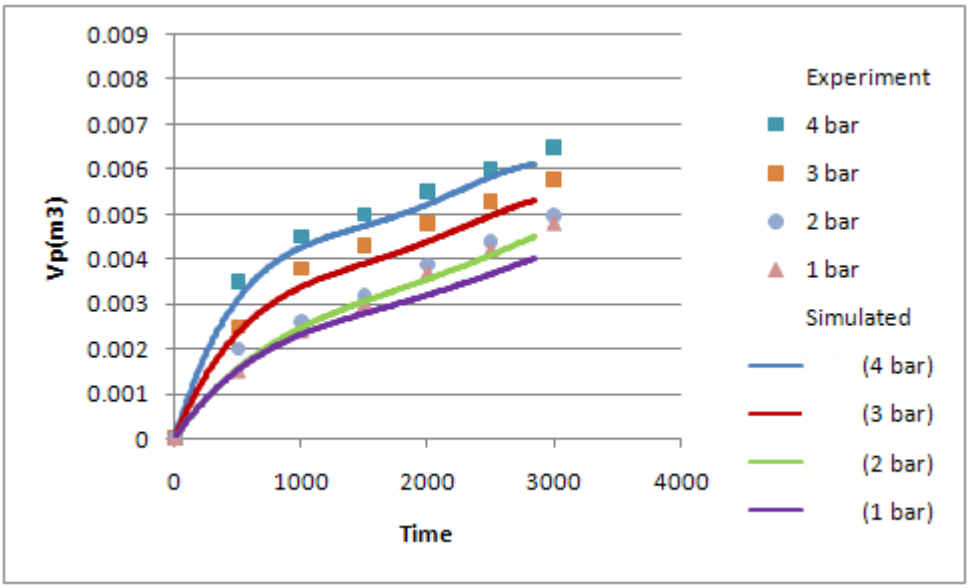

Figure (4.16): Total permeate volume against filtration time at different transmembrane pressure.

2. Different feed flowrate.

Figure (4.17) represents the permeate flux at different feed flow rates (3 to 7 m3/hr). The transmembrane pressures as will the bulk concentration were kept constant at (4 bar) and (5720 mg/L) respectively. As can be seen from Figure (4.17), the permeate flux increased with increasing the feed flow rate due to the same reason has been mentioned previously that the high flowrate reduce the deposition of the solutes that may affect the permeate flux, resulting in the higher permeate flux. In contrast, operating at high feed flow rate could be minimized the concentration polarization effect.

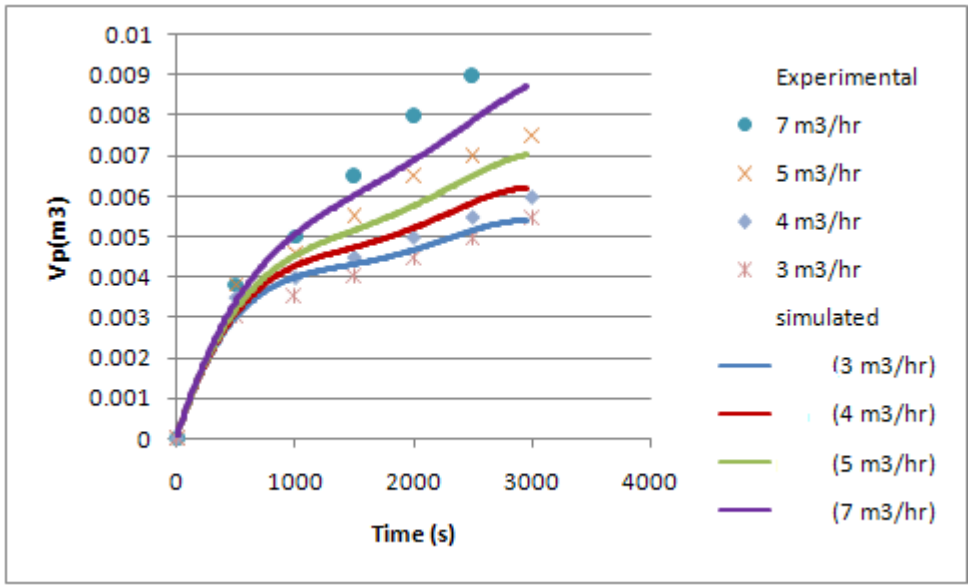

Figure (4.17): Total permeate **v**olume against filtration time at different feed flowrate.

3. Different bulk concentration.

The effect of the bulk concentration on the total permeate at constant transmembrane pressure (4 bar) and constant feed flowrate (4 m3/hr) is shown in Fig(4.18). The decrease in total permeate with time as increase the bulk concentration is due to the formation of cake layer on membrane surface caused by the greater solutes deposition on the membrane surface. The cake layer formed on the membrane surface increased as the amount of the retained solute increases with time.

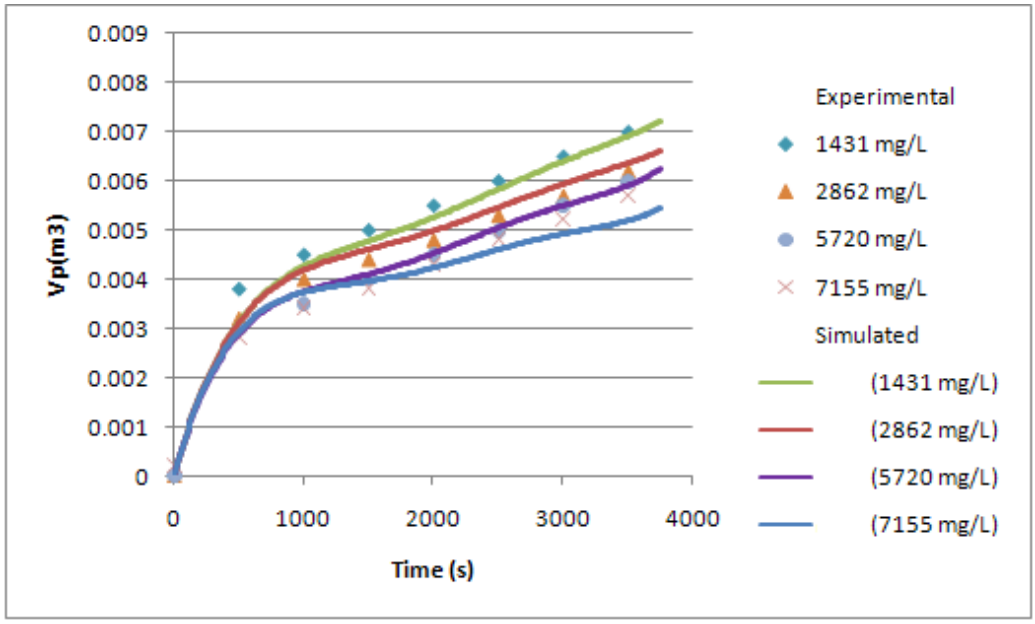

Figure (4.18): Total permeate **v**olume against filtration time at different bulk concentration.

4.4 Comparison between two advanced models

In the previous sections of this Chapter, we looked in particular at various preliminary models that are simplified models (a) osmotic pressure controlled, (b) gel polarization controlled and (c) Gel-layer resistance model. We examined the ability of these simplified models in describing the dynamics of flux decline in ultrafiltration. In the section 4.4.1, the same type of analysis will be repeated for advanced models of flux decline in ultrafiltration. Such advanced models are more complicated that the previous preliminary models since they consist of a complex system of ordinary equations (ODEs) that require the use of a numerical solver. There are two advanced models that will be compared here:

(i) Model 1: Advanced mode that treats the feed solution as multiple-solute feed solution (Ahmed et al.,2006)

(ii) Model 2: Advanced mode that treats the feed solution as a single-solute feed solution (Bhattacharjee and Datta,2003)

The differences between these two advanced models are summarized in Table 4.1.

Table 4.1: The difference between these two advanced models.

Developed model (Multiple - solutes system model) (Ahmed et al.,2006)	***Single -solute system model*** (Bhattacharjee and Datta,2003)
Predict the concentrations of each solute in the permeate.	Predict the total permeate concentration of the system.
The individual mass transport of each solute is important.	The mass transfer coefficient for the mixture. $k_{mixture} = (xk)_{Carbohydrate} + (xk)_{Protein} + (xk)_{Ammonical\ nitrogen}$

4.4.1 Comparison between single solute model and the multi-solute model.

As shown previously, a mathematical model suitable for the multiple solutes system in continuous cross-flow ultrafiltration is developed. This model is suitable to predict the performance of ultrafiltration with multiple solutes system. In this section, we will investigate the capability of the model in predicting the behavior with the single solute system by comparing ultrafiltrate total permeate volume of multiple solute system with single solute system.

Since we deal the multiple solutes system as single solute system we used the mass transfer coefficient for the mixture instead of using the three individual mass transport coefficients for the three solutes (carbohydrate constituents, crude protein and ammonical nitrogen) and the same for the total back transport coefficient.

The two advanced model were compared as seen in the following Figures (4.19-4.24). For all cases the curves for the total volume of permeate of single-solute system demonstrates a similar trend with the total volume of permeates of the multiple solutes system and visually they may look the same. Thus, treating the multiple system as single system slightly influences the total permeate volume.

However, if we take the difference between both curves. (Curve 1(multiple solute system) -Curve 2 (single solute system) we can see that the difference increases progressively with time, since the behavior of a single component system is different from multiple solutes system at later stages when the fouling layer is formed. Another reason is that for the single solute system the model predict the total permeate concentration of the system and not for each individual solute like the multiple solute system. Of course the magnitude of difference is dependent upon the conditions.

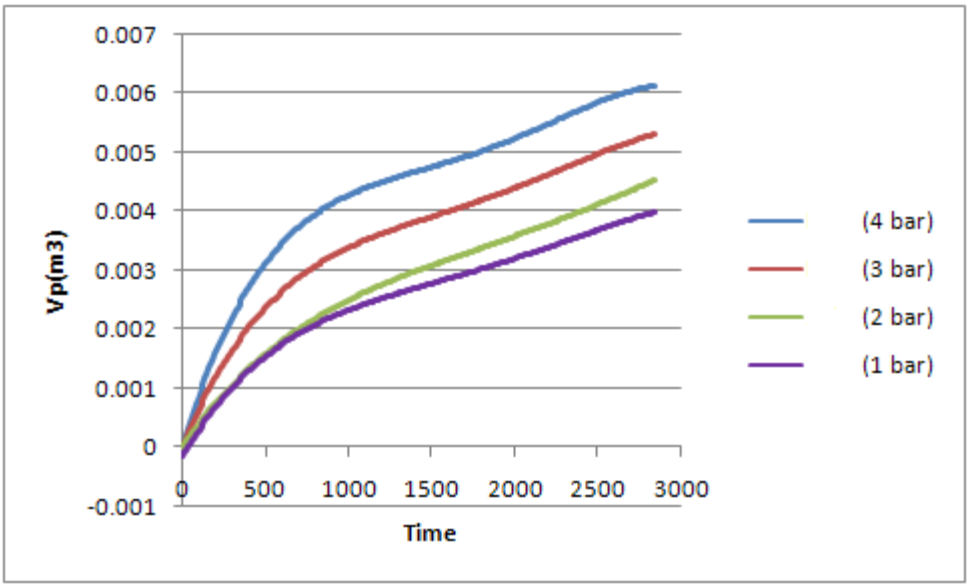

Fig(4.19): Total permeate volume of predicted by an advanced mode that treats the feed solution as multiple-solute feed solution (Ahmed et al,2006) plotted against time at different transmembrane pressures.

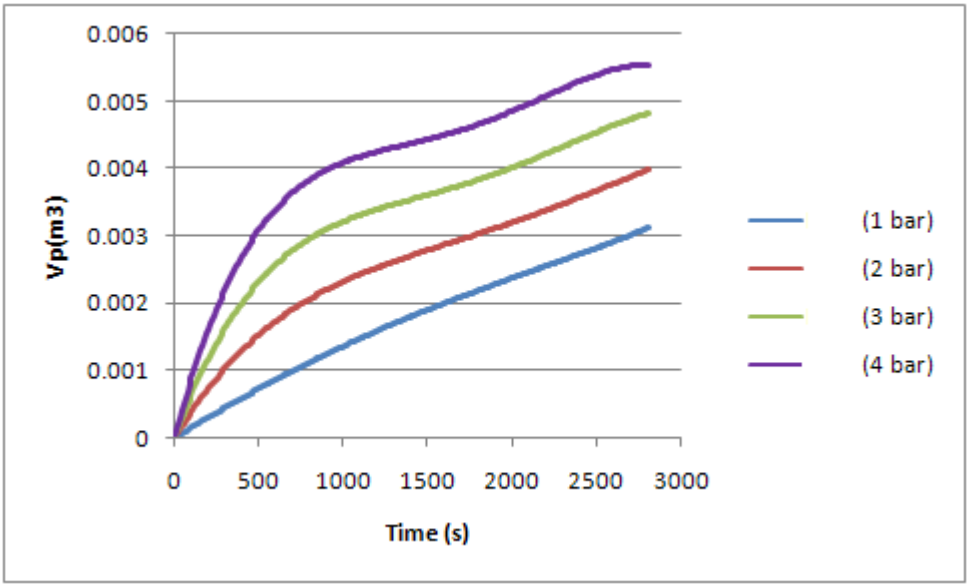

Fig (4.20): Total permeate volume of predicted by an advanced mode that treats the feed solution as a single-solute feed solution (Bhattacharjee and Datta,2003) plotted against time at different transmembrane pressures.

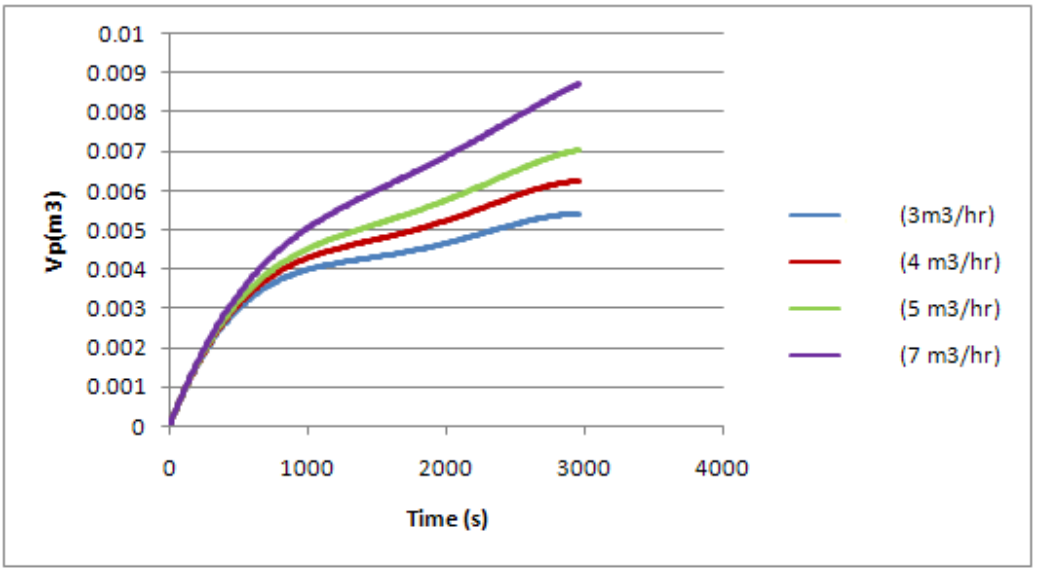

Fig(4.21): Total permeate volume of predicted by an advanced mode that treats the feed solution as multiple-solute feed solution (Ahmed et al,2006) plotted against time at different feed flow rates.

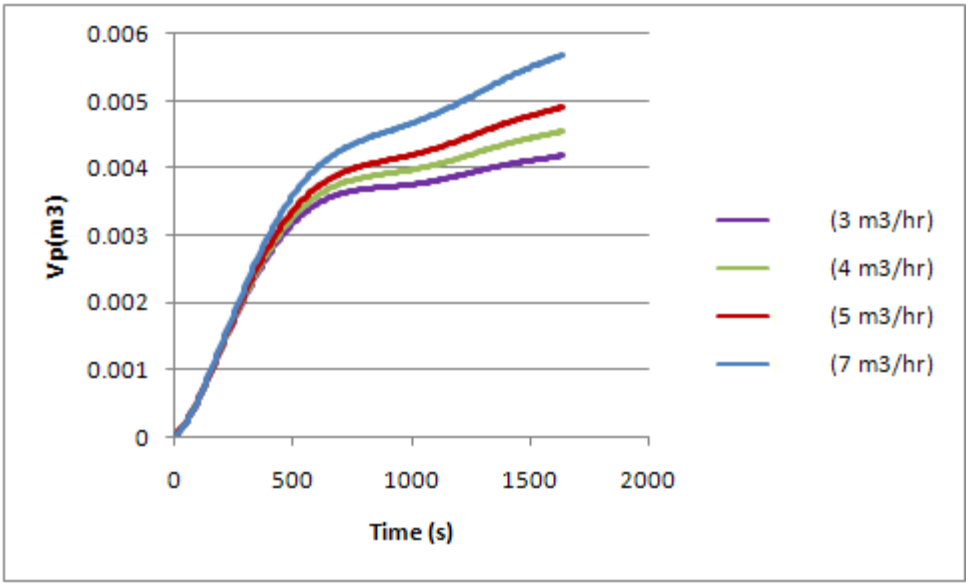

Fig (4.22): Total permeate volume of predicted by an advanced mode that treats the feed solution as a single-solute feed solution (Bhattacharjee and Datta,2003) plotted against time at different feed flowrate .

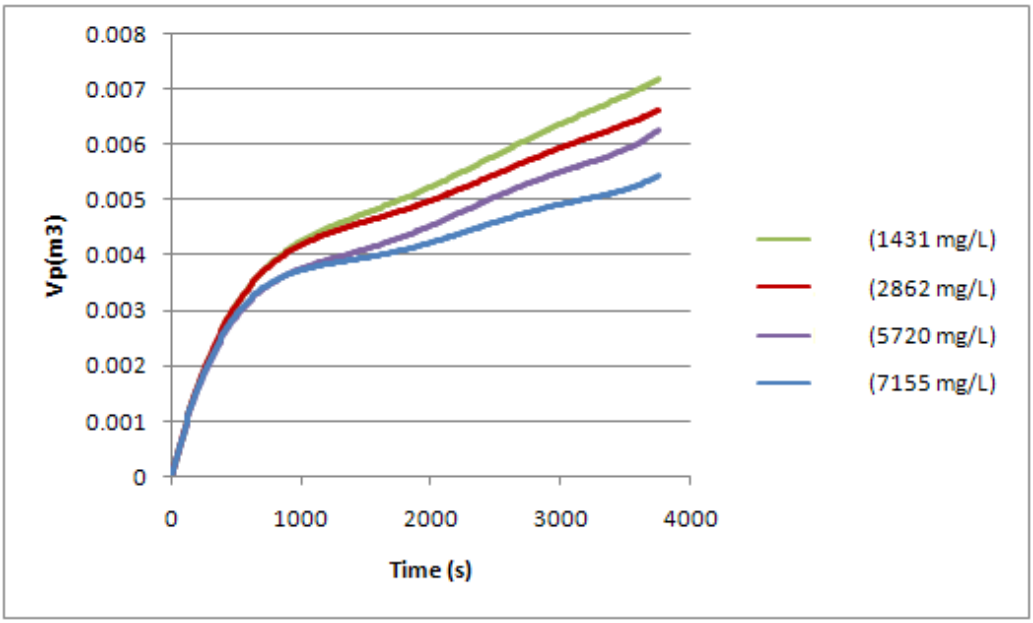

Fig(4.23): Total permeate volume of predicted by an advanced mode that treats the feed solution as multiple-solute feed solution (Ahmed et al,2006) plotted against time at different bulk concentration.

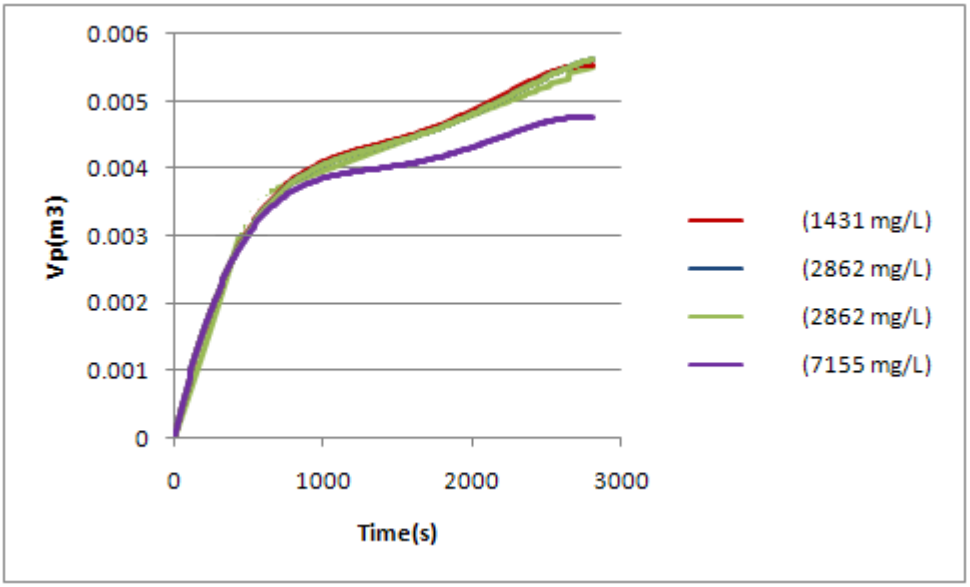

Fig (4.24): Total permeate volume of predicted by an advanced mode that treats the feed solution as a single-solute feed solution (Bhattacharjee and Datta,2003) plotted against time at different bulk concentrations .

CHAPTER 5

Sensitivity analysis with respect to important model parameters.

5.1. Introduction

Flux decline and total volume of permeate in continuous cross-flow membrane ultrafiltration of multiple solute system under various conditions was investigated in Chapter (4). By comparing theoretical predictions with experimental data, it is observed that the permeate flux and the total volume of permeate in continuous cross-flow ultrafiltration is controlled by the dynamic process of cake layer formation and growth. The permeate flux declines with time when the cake layer grows, whereas it attains steady state as the cake layer reaches the equilibrium thickness.

Herein, there are several parameters that can affect the performance of an ultrafiltration system and it is important to know the effect of these parameters on membrane flux since being able to predict the volume flux of permeate (and therefore the flux decline) with time under different parameters will help in design and optimization process.

In order to demonstrate the impact of the parameters on ultrafiltration performance we should return back to the (Ahmad et al., 2006) model

equations that was described in (chapter 4). We mentioned that the usage of eqs (4-17)-(4-20) is to find the permeate volume flux in the multiple solutes system of the continuous cross-flow ultrafiltration and the permeate volume is characterized by the parameters R_m, P_m, K_b, K_{bi} and k_i.

5.2. Key Parameters Influence:

In this section, the ability of development model to predict the effects of changing the system parameters on the volume flux of permeate was investigated. (Ahmad et al., 2006) used the experimental data (chapter 3) to estimate the model parameters. These parameters have been used as base case values as shown in Table 5.1.

Table 5.1: Estimated parameters for the model.

Property	Symbol	Units	Value
Bulk viscosity	μ	$Pa.s$	1.024×10^{-3}
Membrane resistance	R_m	m^{-1}	2.1576×10^{12}
Permeability coefficient	P_m	m^2	8.6464×10^{-16}
Total back transport coefficient	K_{bi}	m^2	
Carbohydrate			19.2414×10^{-8}
Protein			4.3795×10^{-8}
Ammonical nitrogen			8.3812×10^{-8}
Mass transport coefficient	K_h	m/s	4.33×10^{-10}
Carbohydrate			$4.994\times10-^{6}$
Protein			2.9375×10^{-6}
Ammonical nitrogen			3.5777×10^{-6}

We examined the effect of varying: The bulk viscosity, membrane resistance, permeability coefficient, and total back transport coefficient on the total volume of permeate (V_p).

5.2.1. Bulk viscosity :

Since the solution viscosity has an important influence on the ultrafiltration process. The effect of pretreated POME viscosity on total permeates volume in the multiple solutes system of the continuous cross-flow ultrafiltration was studied. Based on Eq. (4.20) the value of total volume of permeate is reduced with rising the viscosity. The influence of viscosity on total volume of permeate is present in Fig (5.1). The figure shows the total volume of permeate versus filtration time with the increasing solution viscosity varying from (1.0244×10^{-7} to 2.25×10^{-7} bar.s). Where it can be seen that there is a substaintial difference in increasing the viscosity on the total volume of permeate .Since increase the solution viscosity have an adverse affect on membrane flux and concentration polarization which also negatively affects total volume of permeate.

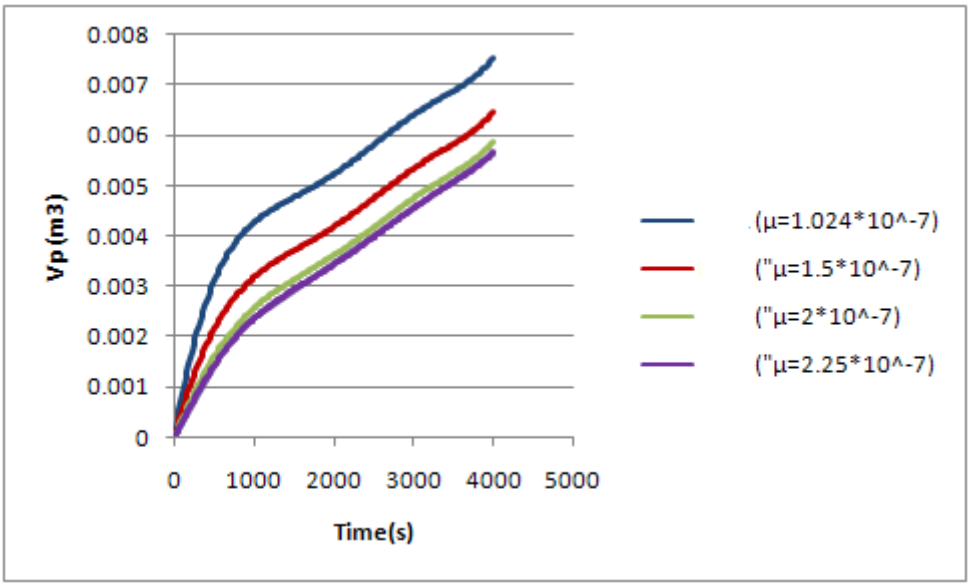

Figure (5.1): Effect of increasing the viscosity on the total volume of permeate. The Other parameters are the same as those given in Table 5.1

5.2.2. Effect of membrane resistance

In membrane operation one of the most important parameters is the membrane resistance which is a measure of the hydraulic resistance to flow through a pore channel and is an intrinsic material property of the membrane. The relationship between the permeate volume and membrane resistance in multiple solutes system of the continuous cross-flow ultrafiltration was investigated via numerical simulations. The volume of permeate could be affected by any changes in membrane resistance.

Fig. 5.2 shows the total volume of permeate versus filtration time with the increasing membrane resistance varying from ($1.024x10^{-7}$ to $2.25x10^{-7}$ m-1).

The result show that the permeate volume decreased when the membrane resistance increased according to eq (4.20) which state that permeate flux across the membrane is directly proportional to the transmembrane pressure and membrane area, but is inversely proportional to the membrane resistance and feed viscosity. The influence of the membrane resistance is more pronounced at the early stages of membrane filtration as seen in Fig 5.2. The values of all parameters used in the simulations shown in Fig. (5.2) were kept constant and similar to those in table 5.1.

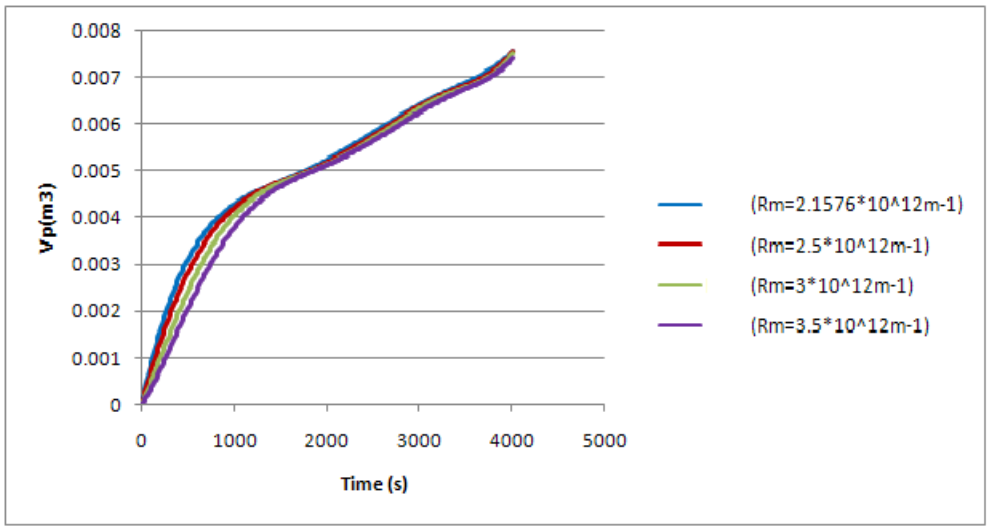

Figure (5.2): Effect of increasing the membrane resistance on the volume flux of permeates.

5.2.3. Effect of permeability coefficient :

In the present study, the permeability coefficient (P_m) of the system depends on both the type of membrane used and the solutes and it was found (

P_m) is equal to 8.646x10^{-16} m2 value as shown in table 5.1. The permeability coefficient (P_m) is a quantitative estimate of the rate of passage of a solute across a membrane (Michael Allaby, 1999)

Figures (5.3) present the influence of permeability coefficient on permeate volume with the increasing the permeability coefficient varying from 8.6464x10^{-16} m2 to 25x10^{-16} m2. It can be observed from this figure that permeate volume increases as permeability coefficient increases and the explanation for this increase in the total volume of permeate is due to the increased permeability coefficient of membranes that permits larger amounts of ultrafiltration and therefore an increased on the total volume of permeate.

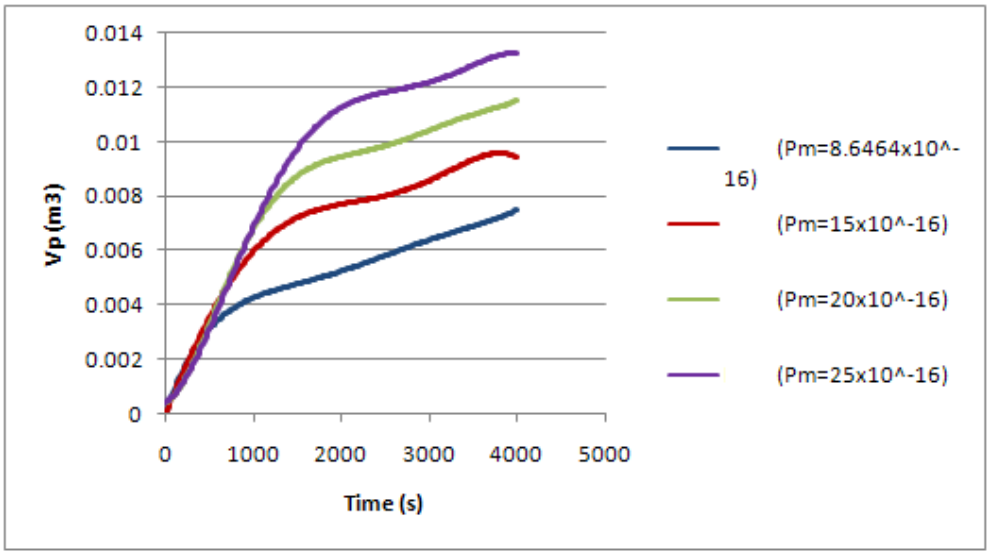

Figure (5.3): Effect of increasing the permeability coefficient on the total volume of permeate. Other parameters are the same as those given in Table 5.1.

5.2.4. Effect of back transport coefficient:

Previously on chapter (4) we have mentioned the back transport coefficient K_b and we said that due to cross currents caused by the superficial velocity, some solutes are removed from the membrane surface and go into the bulk known as back transport effect (back transport coefficient).

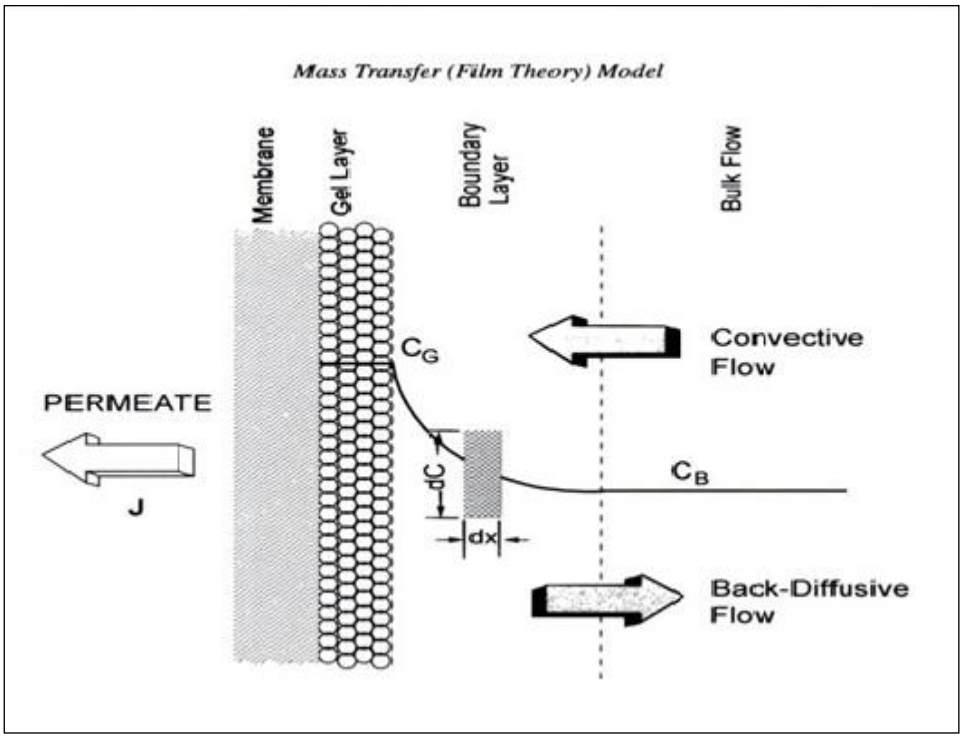

Fig (5.4): Schematic of concentration polarization during UF.(the figure was taken from ultrafiltration and microfiltration handbook by Munir Cheryan).

Fig (5.4) showed the convective transport to the membrane surface is balanced by the back transport from the membrane surface to the bulk. This

back transport is governed by diffusion and it was found that the back-transport of for each solute i is proportional to both the superficial velocity, v ,and the concentration of the solute in the gel layer, C_{gi} and it was found that K_b exhibits a close relationship with the mass transport coefficient k (describe the solutes transport in the gel layer based on the concentration gradient Ahmad A.L 2006). So back transport coefficient plays significant role in explaining the ultrafiltration process. Numerical simulations of the model equations under different back transport value have been attempted in order help to investigate the influence of increasing the back transport coefficient on the total volume of permeate.

Simulations indicate that the increase of the back transport coefficient caused the total volume of permeate to increase. The causes of this increase due to the fact that increase K_b will decrease the concentration of the solute at the membrane surface also decrease the osmotic pressure at the membrane surface (JI), which will increase the driving force (P-JI), which will lead to increase the flux which mean increasing on the total volume of permeate.

The reason for this is explained in the following paragraphs. Where Figure 5.5, Figure 5.6 and Figure 5.7 depicts the variation of the total volume of permeate with increasing the total back transport coefficient under the same parameters as those given in (Table 5.1)**.**

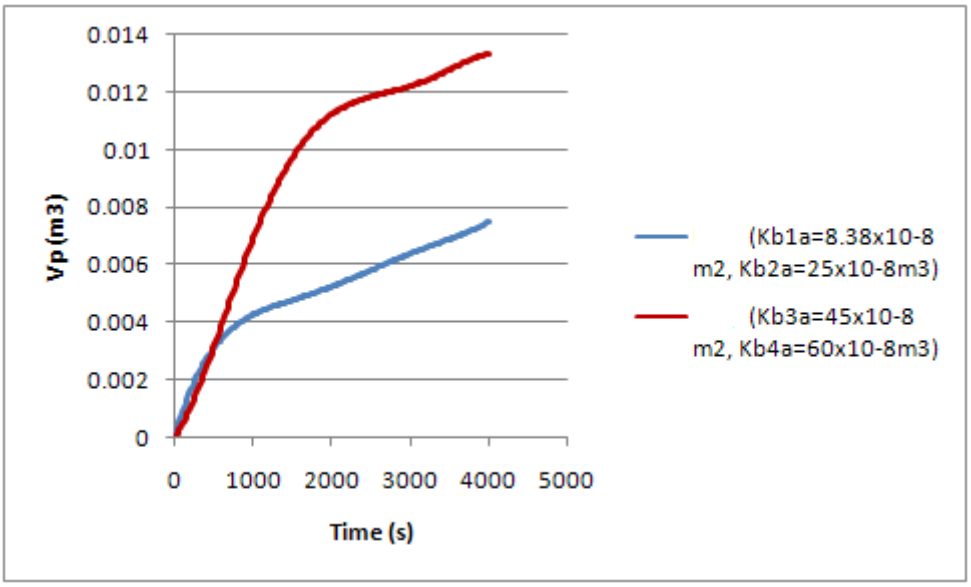

Fig (5.5): Effect of increasing the back transport coefficient of Ammoniacal nitrogen on the total volume of permeate. Other parameters are the same as those given in Table 5.1.

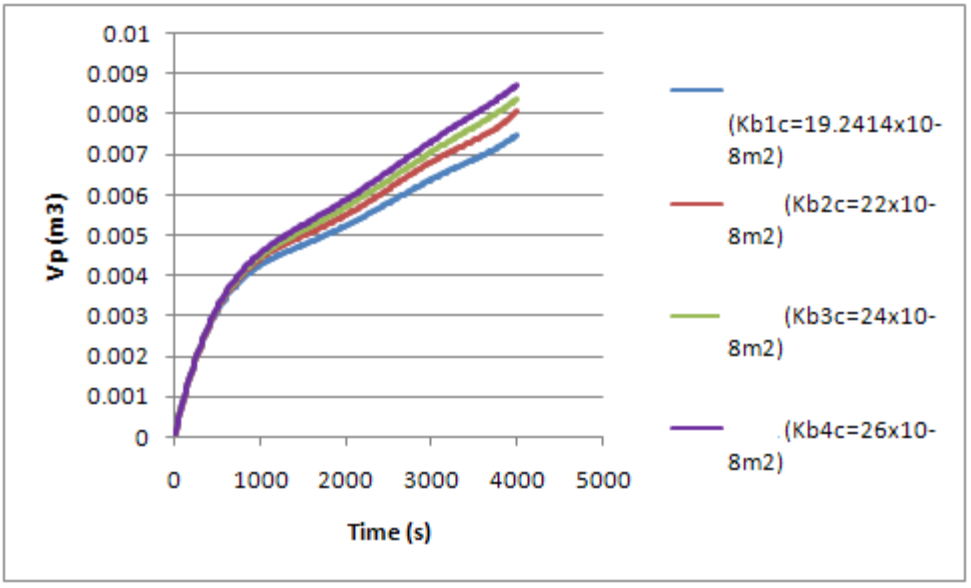

Fig (5.6): Effect of increasing the back transport coefficient of Carbohydrate constituents on the total volume of permeate. Other parameters are the same as those given in Table 5.1.

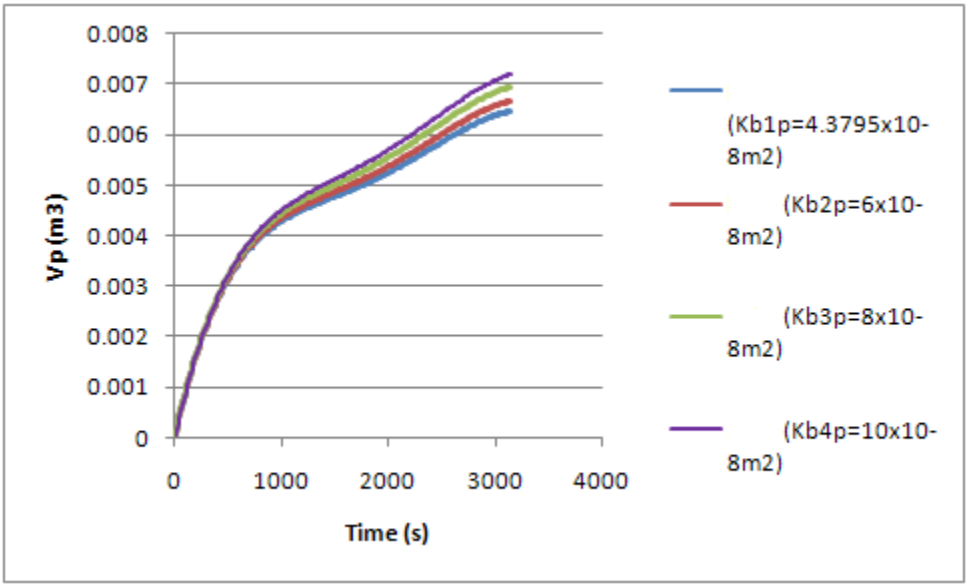

Fig (5.7): Effect of increasing the back transport coefficient of Ammoniacal nitrogen on the total volume of permeate. Other parameters are the same as those given in Table 5.1.

5.3. Summary:

We observed that the bulk viscosity; the membrane resistance , the permeability coefficient and the back transport coefficient parameters affect the dynamics of the ultrafiltration process since the result showed that these model parameters have a significant influence on the total volume of permeate and the permeation flux .

We didn't investigate the effect of increasing the mass transport coefficient k because as mentioned previously, the mass transport coefficient k exhibits a close relationship with the back transfer coefficient K_b . When the mass transport coefficient k increase the back transport coefficient K_b will increase as the well.

CHAPTER 6

Conclusions

This research addresses the attempt to compare the effect of different mathematical models on the ultrafiltration performance of the multiple solute system. The difference in performance can be related to the fouling of the membrane which causes the permeate flux decline with time. Therefore, being able to choose the suitable model is of great interest for both the optimization need and process design in order to help select the model that minimize flux decline with time.

6.1 Contributions

The key contributions of my thesis can be summarized as follows.

Analysis and Comparisons of simple ultrafiltration models (Chapter 4). I discussed the similarities and the differences between various ultrafiltration models (the osmotic model, the gel layer model and the resistance model) under various operating condition (transmembarane pressure, feed flowrate and bulk concentration). The validity of models has been tested by comparing the experimental data presented in Chapter 3 with theoretical predictions of these

models. For the osmotic pressure model (Goldsmith et al.) is one of the pioneers to support the assumption of a possible effect of the osmotic pressure of macromolecular solutions during ultrafiltration. He experienced the effect during ultrafiltration of PEG-15500 and felt that the decrease in permeate flux is due to the increased osmotic pressure produced at the membrane surface because of the rise in concentration of the rejected solute near the membrane surface, using osmotic pressure model (Bhattacharjee et al.). Early study done by Tung-Wen Cheng and Jen-Guo Wu (2001). In their work, they compared between the fluxes predicted by the osmotic-pressure model and the boundary-layer resistance model .Ultrafiltration experiments were conducted in a hollow-fiber membrane module with dextran T500 aqueous solution as tested solution (Tung and Jen (2001)).

For my thesis, I conclude that the resistance model showed closer agreement with the experimental data than both the osmotic and the gel models since the individual osmotic pressure model and the gel layer model are found to be inadequate.

On the other hand I have found that the comprehensive model combining the three models (the osmotic model, the gel layer model and the resistance model) can result in an improvement and reliable prediction of the flux.

Advanced model (Chapter 4). Also I did analysis and comparisons between two advanced models from the literature. The first model was (Ahmad et al., 2006) model where his model was able to predict the performance of continuous cross-flow ultrafiltration process with multiple solutes system and the second model was a unified model (Bhattacharjee et al., 1996)model where this unified model is suitable to predict the performance of batch cell ultrafiltration process with single solute system. Bhattacharjee did analysis of the flux decline encountered during ultrafiltration in batch cell. His analysis was presented by unifying the effluence of the osmotic pressure model and the gel layer model. Bhattacharjee experiments were performed in a batch cell with polymeric solutes (PEG, dextran and PVA) and protein (BSA) under various operating conditions.

In order to have a single solute system I treated the multiple solutes system as single solute system by using the mass transfer coefficient for the mixture instead of using the three individual mass transport coefficients for the three solutes (carbohydrate constituents, crude protein and ammonical nitrogen) and the same for the total back transport coefficient. My results demonstrate that ultrafiltration models that don't explicitly account for multiple solutes system seem to give accurate prediction of total permeate volume and flux decline during the early stages of ultrafiltration.

Study of important model parameters (Chapter 5). Finally, I have used the developed model to investigate the effect of varying the key parameters of the process on the ultrafiltration dynamics and on the volume flux of permeate under different operating conditions (transmembarane pressure, feed flowrate and bulk concentration) since being able to predict the volume flux of permeate (and therefore the flux decline) with time under different parameters will help in design and optimization process. I found that the bulk viscosity, the membrane resistance , the permeability coefficient and the back transport coefficient parameters affect the dynamics of the ultrafiltration process since the result showed that these model parameters have a significant influence on the total volume of permeate and the permeation flux .

My work and Ahmad et al. work is somewhat similar to that considered by Bhattacharjee and Sakar (2006), where they first estimated Different solute–membrane parameters like solute permeability (Pm) and reflection coefficient (σ) based on the theories derived from irreversible thermodynamics. Kedem–Katchalsky (KK) and Spiegler–Kedem (SK) models, from irreversible thermodynamics, were utilized for the parameter estimation and this estimation method some how similar to Ahmad el at. Work were he used the same approach to find the model parameters then Bhattacharjee and Sakar (2006) investigated the variations of solute–membrane parameters like solute permeability (Pm) and reflection coefficient (σ) with other process variable like bulk concentration, pressure difference and stirrer speed. Finally, a three-

parameter simulation model was developed based on film theory, osmotic pressure model and KK/SK models, which were capable to predict permeate flux at any operating conditions. The results of simulation studies were compared with experimental results. Finally, Variation of permeate flux from different models and from experiment as a function of time at different operating condition were studied .

Future Research

There are a number of future research directions suggested by the work in this thesis.

1) Improve (Ahmad et al., 2006) model: Since his model was unable to account for the effects of solute-solute interactions on mass transport in multi-solute system. We have to develop a generalized framework for multi-solute mass transfer that includes solute-solute interaction since solute interactions affect the outcome of ultrafiltration operations and the limiting flux.

2) Improvement the ultrafiltration rejection**:** One possible future research for Ahmad work is to increase the ultrafiltration efficiency since on his work the ultrafiltration gave low rejection of the ternary system (carbohydrate constituents, crude protein and ammonia) and therefore low efficiency of COD. We cane increase the efficiency by using multiple membrane system or by using different membrane modules.

References

Ahmad, A.L., Chong, M.F. and Bhatia, S. (2006), "Ultrafiltration modeling of multiple solutes system for continous cross-flow process",Chemical Eng. Sci, Vol 61, pp.5057-5069.

Baldwin, D.F., Park, C. and Suh, N.P. (1998), "Microcellular Sheet Extrusion System Process Design Models for Shaping and Cell Growth Control", Polym. Eng. Sci, Vol 38 (4), pp.674-688.

Bhattacharjee,S. ,Sharma A. and Bhattacharya, P.K. (1996). "A unified model for flux prediction during batch cell ultrafiltration ", Chem.Eng.Sci., Vol.52 (4), pp.627-633.

Sablani, S.S. (2007), "Handbook of food and bioprocess modeling techniques", Food Science and Tech., pp. 135-230.

Cheryan M. (1998), "Ultrafiltration and microfiltration handbook study of bubble growth during low pressure structural foam molding process", Second edition, pp.115-128.

Yun-ren, Q., Hong, z., Qui-xiu, Z. (2009), "Treatment of stable oil/water emulsion by novel felt-metal supported PVA composite hydrophilic membrane using cross flow ultrafiltration" Science Direct, Vol.(19), No.(3), pp.773-777.

Hameed, B.h., Ahmad, A., Hoon, N.A(2003), “Removal of residual oil from palm oil mill effluent using solvent extraction method ”, Jurnal Teknology, 38(F), pp.33-42.

Kedem,O., and Katchalsky, A. (1961), “A physical Interpretation of the Phenomenological Coefficients of Membrane Permeability ”,The Journal of General Physiology.Vol 45, 143-179.

Jonsson ,G. (1986), “Transport phenomena in ultrafiltration : membrane selectivity and boundary layer phenomena ”, Pure &AppI. Chem.,Vol.58 (12), pp. 1674-1656.

Vela, M.C.V, Blanco, S.A. and Garcia, J.L. (2005) “Crossflow ultrafiltration of cake forming solutes: a non-steady state model ”, Desalination 148 pp. 347-356.

Vela, M.C.V, Blanco, S.A. Garcia, J.L. and Rodriguez E.B (2008) “ Fouling dynamics modeling in the ultrafiltration pf PEGs ”, Desalination 222 ,pp. 451-456.

Vela, M.C.V., Blanco, S.A. Garcia, J.L. and Rodriguez E.B (2005), “Permeate flux decline prediction in the ultrafiltration of macromolecules with empirical estimation of the gel layer concentration”, Desalination 221, pp.390- 394.

Mohammadi, T., Khopeyma, A. and Sadrzadeh, M. (2008) “Mathmatical modeling of flux decline in ultrafiltration ”, Desalination 184 ,pp. 367-375.

Foley, G. (1999), “Minimisation Of Process Time In Ultrafiltration and Continous Diafiltration: The Effect Of Incomplate ”, Journal of Membrane .Sci. 163, 349-355.

Goosen, M.F.A., Sablani, S.S., Al-Hinal, A., Al-Obeidani S.,Al-Belushi R., and Jackson, D., (2004), “Fouling of Reverse Osmosis and Ultrafiltration Membrane: A Critical Review” ,Separation Science and Technology Vol.39(10), pp. 2261-2298.

Wei, D.S., Hossain, M. and Saleh, Z. S. (2007) “Separation of Polyphenolics and Sugar by Ultrafiltration: Effects of Operating Conditions on Fouling and Diafiltration” World Academy of Science, Engineering and Technology 34, pp.17-24.

Vela, M.C.V., Blanco, S.A. Garcia, J.L. and Rodriguez E.B (2007), “Validation of Dynamic Models to Predict Flux Decline in the Ultrafiltration ”, Desalination, 204,pp.344-350.

Vela, M.C, Cook, R.F., and Macosko, C.W. (2005), “ Qualification of Flux Decline of Depectinized Mosambi (CITRUS SINENSIS[L.] Osbeck) Juice

Using Unstirred Batch Ultrafiltration ", Journal of Food Process Engineering ,**28**, pp.359-377.

Salgin, U. and Salgin, S. (2007), "Crossflow Ultrafiltration of Binary Biomolecule Mixture: Analysis of Permeate Flux, Cake Resistance and Sieving Coefficient", Chem. Eng. Technol. 2007, 30, No. 4, 487–492

Vela, M.C.V., Blanco, S.A. Garcia, J.L. and Rodriguez E.B. (2007), "Modeling of Flux Decline in Cross-Flow Ultrafiltration of Macromolecules: Comparison Between Predicted and Experimental Results". Desalination, 204, pp.328-334.

Limsawat, P. and Pruksasri, S. (2010), "Separation of lactose from milk by ultrafiltration",As. J. Food Ag-Ind., 3(02), 236-243.

Tsapiuk, E.A. (1997), "Calculation of the Product Composition and the Retention Coefficient by Pressure Driven Membrane Separation of Solutions Containting one and Two Solute", J. of Membrane Science., 124, pp. 107-117.

Darnon, E., Belleville, M.M.P. and Rios, G.M.(1996), "Ultrafiltration within Downstream Processing: Some Process Design Considerations", Chemical Engineeringand Process Journal, Vol.42.pp.299-309.

Bowen, W.R., Cao, X. and Williams ,P.M. (1995), "Use and Elucidation of Biochemical Data in the Prediction of the Membrane Separation of Biocolloids", Proc.R. Soc. Lond. A 455, pp.2933-2955.

Bowen, W.R., and Jenner F. (1995). “Theoretical Descriptions of Membrane Filtration of Colloids and Fine Particles: and Assessment and Review ”. Advances in Colloid and Interface Science ,56 pp. 141-200.

Mohammadi, T. and Esmaeelifar, A. (2004), “Wastewater treatment Using Ultrafiltration at a Vegetable Oil Factory” Desalination, Vol. 166, pp. 329-337.

Zhang, J.C. Wang Y.H. Song,L.F. Ng, W.J. and Lee,L.Y. (2005), “Feasibility Investigation of Refinery Wastewater treatment by Combination of PACs and Coagulant with Ultrafiltration ”, Desalination, Vol. 174, pp. 247-256.

Vela, M.C.V., Blanco, S.A. Garcia, J.L. and Rodriguez E.B. (2006), “Application of a dynamic model for predicting flux decline in crossflow ultrafiltration”, Desalination, Vol. 198, pp. 303-309.

Serra,C., Koelling, K.W., Clifton,M.J., Moulin, P. Rouch, J.C. andAptel, P. (1998), “ Dead-end ultra®ltration in hollow Fiber modules: Module design and process simulation”, J. of Membrane Science., 145, pp. 159-172.

Teodosiu, C. and Barjoveanu, G. (2010), “Modeling and Simulation of An Ultrafiltration Process for the removal of Suspended solids and Colloids from

Wastewater ", Environmental Engineering and Management Journal, Vol. 9 (3), pp.361-371..

Nobel, R.D., Stern, S.A. (1995), "Membrane Separations Technology: Principles and Applications ",Membrane Science and Technology Series, 2. 1st edition.

Song,L. (1999), "A New Model for the Calculation of the Limiting Flux in Ultrafiltration". J. of Membrane Science , Vol.(144), pp. 173-185.

Ali, M.S.A. (2005), "Development of Integrally Skinned Polysulfone Ultrafiltration Membrane: Effect of Casting Parameters ", Master thesis, pp. 280.

Drioli, E., Curcio, E. and Fontananova, E., "Mass Transfer Operation-Membrane Separations ",In. on Membrane Technology , Dep. Of Chemical Engineering and Materials , University of Calabria, Italy .

Berg, G.B.V., and Smolders C.A. (1990), "Flux Decline in Ultrafiltration Processes", Desalination,77 pp. 101-133.

Saksena, S. and Zydney A.L. (1998),"Influence of protein-protein interactions on bulk mass transport during ultrafiltration ", Journal of membrane science,Vol.125(1) pp.93-108.

Stoner,M.Ficher N. Nixon, L. Benke, M. Austin F. and Favelukis, M. (2004),"Protein–solute interactions affect the outcome of ultrafiltration/diafiltration operations", Journal of Pharmaceutical science,Vol.93(9). pp.2332-2342.

Shen, J.J.S. and Probstien ,R.F.(1977), "On the Prediction of Limiting Flux in Laminar Ultrafiltration of Macromolecular Solutions", *Ind. Eng. Chem. Fundamen*, Vol.16(4), pp.459-465.

Sethi, S., and Wiesner, M.(1997), "Modeling of transient permeate flux in cross-flow membrane filtration incorporating multiple particle transport mechanisms",Jurnol of membrane. Sci, Vol 136 (1), pp.191-205.

Goldsmith R.L., (1971) " Macromolecular ultrafiltration with micro porous membranes" Ind. Eng. Chem. Fundam. 10 113–120.

Bhattacharjee C., Sarkar P., S. Datta S., B.B. Gupta B.B., Bhattacharya P.K.. (2006), "Parameter estimation and performance study during ultrafiltration of Kraft black liquor". Elsevier ,Separation and Purification Technology,1-11.